Geological Society of America
Special Paper 307
1996

A model of the Chicxulub impact basin based on evaluation of geophysical data, well logs, and drill core samples

Virgil L. Sharpton
Lunar and Planetary Institute, 3600 Bay Area Boulevard, Houston, Texas 77058-1113
Luis E. Marín
Instituto de Geofísica, Universidad Nacional Autónoma de México, Ciudad Universitaria, Mexico City, CP 04510, Mexico
John L. Carney
Amoco Production Company, 501 WestLake Park Boulevard, Houston, Texas 77253
Scott Lee, Graham Ryder, and Benjamin C. Schuraytz
Lunar and Planetary Institute, 3600 Bay Area Boulevard, Houston, Texas 77058-1113
Paul Sikora
Amoco Production Company, 501 WestLake Park Boulevard, Houston, Texas 77253
Paul D. Spudis
Lunar and Planetary Institute, 3600 Bay Area Boulevard, Houston, Texas 77058-1113

ABSTRACT

Abundant evidence now shows that the buried Chicxulub structure in northern Yucatan, Mexico, is indeed the intensely sought-after source of the ejecta found worldwide at the Cretaceous-Tertiary (K/T) boundary. In addition to large-scale concentric patterns in gravity and magnetic data over the structure, recent analyses of drill-core samples reveal a lithological assemblage similar to that observed at other terrestrial craters. This assemblage comprises suevite breccias, ejecta deposit breccias (Bunte Breccia equivalents), fine-grained impact melt rocks, and melt-matrix breccias. All these impact-produced lithologies contain diagnostic evidence of shock metamorphism, including planar deformation features in quartz, feldspar, and zircons; diaplectic glasses of quartz and feldspar; and fused mineral melts and whole-rock melts. These features indicate a range of peak pressures from <8 GPa to >60 GPa. In addition, elevated concentrations of Ir, Re, and Os, in meteoritic relative proportions, have been detected in some melt-rock samples from the center of the structure. Isotopic analyses, magnetization of melt-rock samples, and local stratigraphic constraints identify this crater as the source of K/T boundary deposits.

Although the size and precise morphology of this buried basin are not yet established conclusively, the evidence gathered to date from geophysical data, well logs, and drill-core samples indicates that the Chicxulub basin may be ~300 km in diameter. Chicxulub's circular gravity depression appears to be nearly 300 km in diameter; at other terrestrial craters the edge of the gravity anomaly roughly coincides with the topographic basin rim. Superimposed on this broad depression are local concentric anomalies consistent with the structure of a multiring impact basin. Depths to the K/T boundary in well logs also are consistent with an ~300-km basin but are not as expected of a crater less than 200 km in diameter. Thus, steep gravity gradients located between 75 to 105 km from center may outline a central region of deep deformation associated with transient crater collapse rather than the final basin rim as previously assumed. Similar steep, inward-facing gradients delimit deep deformation at other terrestrial craters. Well data indicate that the silicate basement within ~160 km of Chicxulub's cen-

Sharpton, V. L., Marín, L. E., Carney, J. L., Lee, S., Ryder, G., Schuraytz, B. C., Sikora, P., and Spudis, P. D., 1996, A model of the Chicxulub impact basin based on evaluation of geophysical data, well logs, and drill core samples, *in* Ryder, G., Fastovsky, D., and Gartner, S., eds., The Cretaceous-Tertiary Event and Other Catastrophes in Earth History: Boulder, Colorado, Geological Society of America Special Paper 307.

ter is ~1 km deeper than in wells farther out. This is consistent with late-stage collapse of the crater flanks to yield a final basin ~300 km in diameter but is hard to reconcile with a much smaller crater. Finally, the ejecta thicknesses exceed 600 m in regions where they previously were estimated to be less than about 90 m. Such observations provide an intriguing—albeit not airtight—case for an ~300-km-diameter multiring impact basin.

BACKGROUND

The buried Cretaceous-Tertiary (K/T) source crater in northernmost Yucatan (Plate 1) was first recognized as a zone of concentric anomalies in gravity surveys circa 1948 (Cornejo-Toledo and Hernandez-Osuna, 1950), prompting an exploratory drilling program by Petróleos Mexicanos (Pemex) that began in the early 1950s. By then, the feature was known as the Chicxulub structure after the small Mayan village of Chicxulub near the structure's center, the place where the first exploratory well was drilled (Antonio Camargo, personal communication, 1994). The Pemex drilling program comprised eight deep holes, with intermittent core recovery, and was completed in the mid-1970s. This effort revealed unusual occurrences of Upper Cretaceous crystalline rocks and breccias—thought at the time to indicate a large volcanic field—amid the typical Mesozoic carbonate platform sequence of this region (Lopez-Ramos, 1983).

Penfield and Camargo (1981) first reported Chicxulub's unusual features and proposed that they could signal a large buried impact structure. Even though popular reports at that time (Byars, 1981; Sky and Telescope, 1982) suggested this could be the elusive site of the K/T impact event proposed by Alvarez et al. (1980), Chicxulub went virtually unnoticed for almost a decade. In the meantime, impact enthusiasts explored various scenarios to mitigate the absence of a recognized K/T crater large enough to account for the environmental crisis predicted by the Alvarez hypothesis. By the second Snowbird meeting in 1988 (Sharpton and Ward, 1990), two potential solutions to this problem had gained broad acceptance: (1) a large K/T impact site on the ocean floor would be difficult to recognize and could have been destroyed during 65 million years of plate recycling; (2) many smaller impact events, occurring either simultaneously or in a narrow time window, could initiate the K/T biospheric crisis without the need for a 200-km-class crater. Both these ideas were convenient and both were seriously considered even though there was very little, if any, robust evidence in their support.

During the last few years, however, as analyses of K/T boundary materials yielded clear evidence of a single (Bohor, 1990) continental impact site (Bohor, 1990; Sharpton et al., 1990a, b; Izett, 1990; Izett et al., 1990), in the vicinity of the Gulf of Mexico (Bourgeois et al., 1988; Hildebrand and Boynton, 1990), attention turned finally toward the Yucatan Peninsula of Mexico (Sharpton et al., 1990b; Hildebrand and Boynton, 1990). Even then, however, the rediscovery of the Chicxulub structure was not a clever act of scientific detective work, as it is sometimes portrayed. As late as 1991, the group conducting the most ambitious search for the K/T crater was still combing ocean floor in the Colombian Basin off the coast of Nicaragua. It took the intervention of Carlos Byars, the reporter for the *Houston Chronicle* who had interviewed Penfield and Camargo in 1981, to put the planetary community on the track to Chicxulub almost a decade later.

Armed with this information, it was only a matter of time until Chicxulub became the center of intense scientific scrutiny; drill core samples were soon located, and a number of laboratories began to uncover more compelling evidence that the Chicxulub structure is a buried impact crater and to strengthen its temporal link to the KT extinction event (Hildebrand et al., 1991; Pope et al., 1991, 1993; Kring and Boynton, 1992; Sharpton et al., 1992, 1993, 1994a, b; Swisher et al., 1992; Blum et al., 1993; Krogh et al., 1993; Koeberl et al., 1994; Schuraytz and Sharpton, 1993; Schuraytz et al., 1994). Focus is now shifting from proving the origin and age of the Chicxulub impact basin to gaining a better understanding of the crater as well as the geological and environmental consequences of the impact event that produced it.

Here we assemble and assess the geophysical and geological characteristics of the Chicxulub basin as understood to date, including the general stratigraphic sequence of impact lithologies and target rocks obtained from drill-core and well-log data. We combine these constraints with those derived from terrestrial and planetary crater studies to construct a general model of the Chicxulub structure as an ~300-km-diameter impact basin and discuss its implications.

THE GEOPHYSICAL EXPRESSION OF THE CHICXULUB STRUCTURE

Morphology and structure of impact-generated landforms

Exploration of the inner solar system during the latter half of the twentieth century has shown that large-body impact played a major role in shaping ancient planetary landscapes such as those preserved on Mercury and the Moon. It is there, on the ancient surfaces of these small airless planets, that the best examples of large impact basins are observed (e.g., Spudis, 1993). The largest basins exhibit multiple concentric rings and can exceed 2,000 km in diameter. In contrast, Earth's active surface processes quickly destroy its impact record; only ~140 impact craters have been identified so far and many are small, bowl-shaped, or simple craters. Larger complex structures, greater than about 4 km in diameter on Earth, are rarer, older, and more modified; the truly large impact basins, those greater than ~50 km in diameter, are extensively modified and have retained few, if any, clues to their original surface configuration. But such erosional and tectonic activity, combined with extensive drilling and geophysical surveys, also affords the only information on crater substructure

from which to understand the third dimension of large impact craters—anywhere in the solar system.

The smallest pristine craters on any planet are simple bowl-shaped depressions with raised rims; these features are produced by the downward displacement and the excavation flowfield initiated by a system of impact-driven compression and rarefaction waves (see Melosh, 1989, for a complete treatment of the physics of impact). But larger-magnitude impacts create transient conditions within the target that initiate large-scale, gravity-driven modification of this bowl-shaped crater form during the final stages of the impact event. Two processes take place immediately and almost simultaneously: The floor of the initial or "transient crater" rebounds upward, producing a central structure that, when exposed, takes the form of a central peak composed of the originally deep target rocks comprising the crater subfloor; and the crater margins collapse inward along either a series of normal faults (producing terraces) or along a single scarplike fault. This late-stage modification results in a final basin that is broader and shallower than the transient crater and is characterized (ideally) by a central peak, broad flat floor deposits, and a terraced rim zone. (N.B.: The "transient crater" is a theoretical construct that aids conceptualization of the cratering process; however, given the scale and complexity of planetary cratering events, there could be considerable overlap in time between excavation and modification, i.e., central rebound may begin prior to the termination of excavation and outward flow at the distal parts of the excavation cavity; consequently a true transient crater may not fully form before modification destroys it.) The modified basin is filled with a mixture of melt rock and highly shocked rock debris, both originating near the impact site, as well as a considerable amount of weakly shocked or unshocked debris, much of which entered the basin during slumping and enlargement. For consecutively larger impact events, the central peak is replaced by clusters of peaks, and finally by a peak ring.

At the very largest diameters, impact basins are characterized by two or more concentric rings in addition to—and outside of—the central peak ring. The canonical multiring basin is the Orientale basin on the Moon (Fig. 1). Multiring basins have been studied intensely over the course of 30 years of planetary investigations (e.g., Baldwin, 1963; Schultz, 1976; Head, 1977; Melosh and McKinnon, 1978; Pike and Spudis, 1987; Melosh, 1989; Spudis, 1993), yet even now they are not well understood. The surficial expression of basin rings, particularly the distal ones, can be quite subtle, especially when the basin has been modified by eons of subsequent geological activity, as most have. There is even debate over whether or not multiring basins exist at all on some terrestrial planets (see discussion in Chapter IX, Melosh, 1989), and one faction maintains that a planetary asthenosphere is necessary for multiring basin formation (Melosh and McKinnon, 1978; Melosh, 1989). This lack of consensus has led to a generally hesitant approach to interpreting even the largest impact features on Earth as the modified remains of multiring basins.

The recent Magellan mission provided the first high-resolution unencumbered views of the surface of Venus. Recognition that multiring basins occur on that planet (Schaber et al., 1992; Alexopoulos and McKinnon, 1994), so different from the Moon and Mercury, yet so similar to Earth in terms of its surface gravity, atmospheric conditions, and target strength, has strengthened the proposition that multiring-basin morphology is an ultimate consequence of increased impact energy and not related to some planetary property such as the presence of an asthenosphere. The diameter at which the transition from peak-ring basins to multiring basins takes place appears to follow the same inverse dependence on planetary gravity as the transition from simple to complex craters and the transition from central-peak to peak-ring basins. All impact basins greater than ~140 km on Venus exhibit the attributes of multiring basins; this and the basic similarities between Venus and Earth suggest that impact features of this size on Earth should correspond to multiring basins as well. Three terrestrial craters identified to date exceed this size: the Sudbury structure in Ontario, the Vredefort structure in South Africa, and the Chicxulub structure.

Gravity data over Chicxulub

Penfield and Camargo (1981) originally recognized two concentric zones in gravity anomaly and aeromagnetic data over the Chicxulub structure: an inner zone ~60 km in diameter, characterized by a local gravity high and high-frequency magnetic anomalies approaching 1,000 nT, and an outer gravity trough with low amplitude (5 to 20 nT) magnetic anomalies. Hildebrand et al. (1991), primarily on the basis of these patterns proposed that the Chicxulub crater was a double-ring or peak-ring basin with a rim diameter of ~180 km. More recently, however, the gravity data over the northern Yucatan have been reprocessed (Sharpton et al., 1993), and additional concentric patterns outside the original two have been identified (Plate 1 and Fig. 2), providing geophysical evidence that the Chicxulub basin is ~300 km in diameter and may be a multiring impact basin.

The gridded Bouguer gravity anomaly map of the Yucatan region is shown in Plate 1B. Gravity anomalies in the vicinity of the Chicxulub basin (Plate 1C) range from −16.4 mgal (10^{-5} m s^{-2}) to +53.6 mgal. The Chicxulub basin is expressed as a broad, nearly circular region in which gravity values are 20 to 30 mgal lower than regional values. A distinct 15- to 20-mgal high occupies the geometric center which we place at 21.3° N latitude and 89.6° W longitude. Figure 2 shows gravity profiles through the center of the structure for each 10° of azimuth and clearly reveals multiple rings expressed as local maxima in the gravity anomaly data. Like topographic rings at large multiring basins on other planets, these rings are spaced systematically such that distances between successive rings are approximately multiples of $\sqrt{2}$ (Pike and Spudis, 1987; Spudis, 1993; Sharpton et al., 1993). Major topographic rings characteristic of multiring impact basins include (1) the innermost or central peak ring, thought to represent the topographic expression of the central uplift (Grieve et al., 1981; Melosh, 1989, p. 163–168).

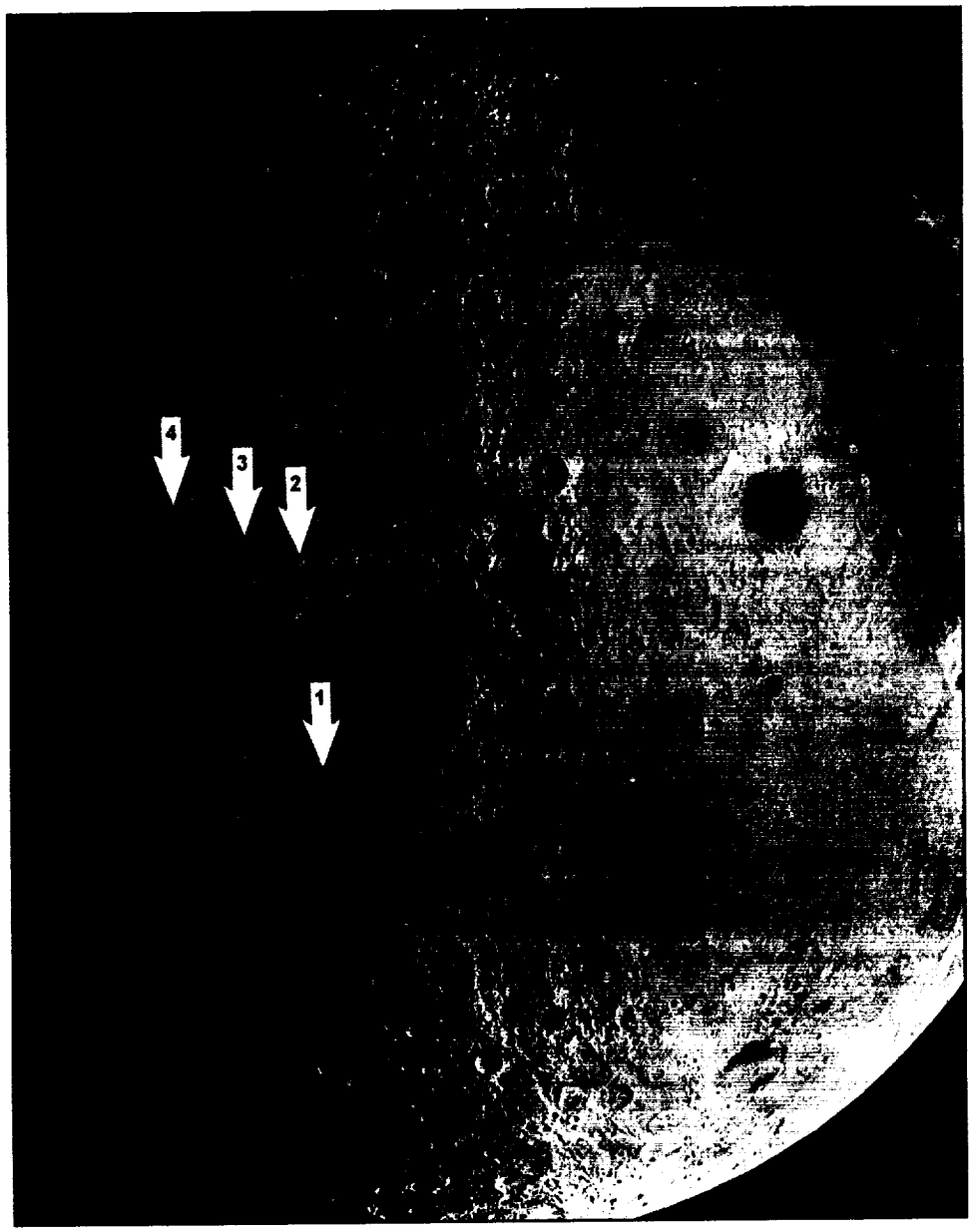

Figure 1. The 930-km Orientale Multiring Basin on the western limb of the Moon as seen from the Lunar Orbiter IV spacecraft. North is toward the top of the page. Numbered arrows indicate the four main basin rings (e.g., Howard et al., 1974; Wilhelms, 1987, Chapter 4, Spudis 1993). 1 is the central peak ring; 2 and 3 are the Inner and Outer Rook Mountain rings, respectively; and Ring 4 is the Cordilleran Scarp.

(2) one or more intermediate rings marking the margins of annular shelves stepping down toward the center, and (3) the topographic basin rim (Spudis, 1993, p. 7, Fig. 1.2).

The central peak ring. The first gravity ring at the Chicxulub structure has a crest diameter of ~100 km and probably corresponds to the central peak ring, that is, equivalent to the innermost ring at the Orientale Basin on the Moon (Ring 1; Fig. 1). In their 170-km-diameter model of the Chicxulub crater, Pilkington et al. (1994) place the central peak ring at the annular low between the central gravity high and this first ring of local gravity maxima. They attribute their ring of local negative anomalies to a thick wedge of low-density breccia that they claim makes up the central peak ring. In their model, this breccia wedge floats on a thick pool of impact melt rock. Such a peak ring—physically decoupled from, and unrelated to, the central uplift—is at odds with all observations of central structures of terrestrial craters (e.g., Howard et al., 1974; Grieve et al., 1981) and evaluation of planetary crater records (Spudis, 1993). From

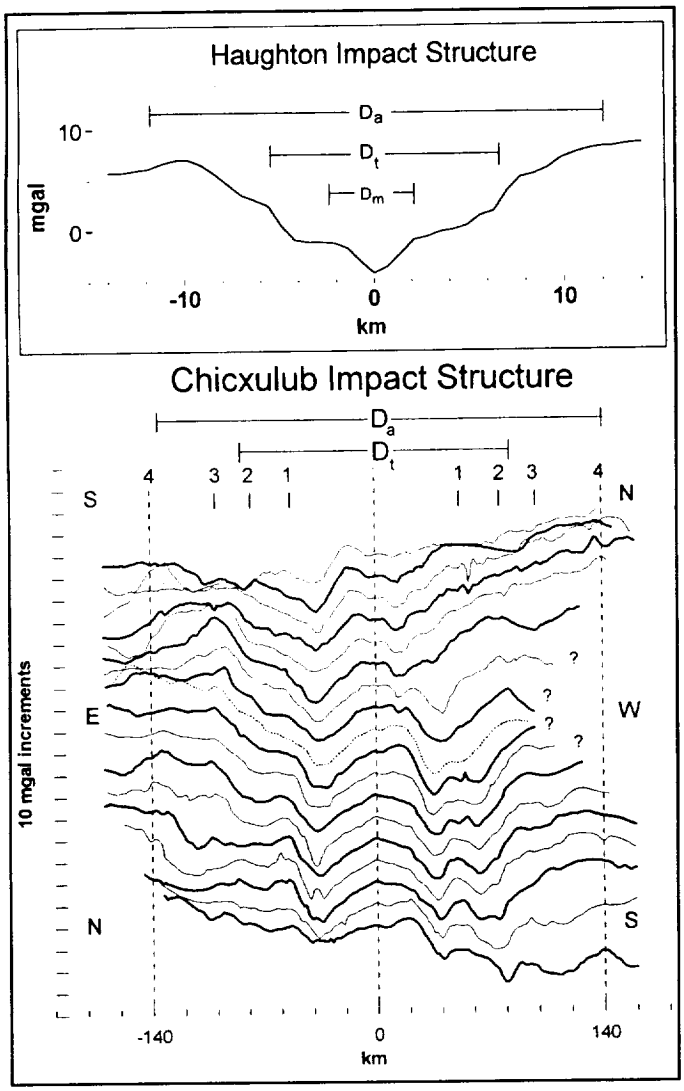

Figure 2. Radial gravity profiles taken across the Chicxulub basin at 10° intervals of azimuth. D_t and D_a refer to the transient crater diameter and final or apparent crater diameter resulting from this analysis. Numbers denote average position of gravity rings shown in Plate 1. Profiles are offset vertically by 10 mgal; the annotated vertical axis shows the 0 mgal value for each profile, beginning from the bottom with N to S. Dashed profile is due E to W. The value of the center point of each gravity profile is 10.4 mgal. Inset: The Haughton impact structure also shows a marked steepening in gravity gradient at the edge of the transient crater. Note also that the zone of intense magnetization is considerably smaller than D_t.

studies of such terrestrial craters as the 100-km-diameter Popigai structure (Masaitis et al., 1980; Masaitis, 1990) and the 24-km-diameter Ries crater (e.g., Pohl et al., 1977) it is well known that the central peak ring is the upper surface of deep crustal massifs that comprise the central uplift. Images of well preserved ring basins on other planets demonstrate that this ring often, but not always, appears as a topographic ring, cropping out through the melt-rock and breccia deposits.

The Sudbury and Vredefort impact structures are both well-studied ancient impact basins interpreted to be between ~180 and 300 km in diameter, and although their outer reaches have experienced considerable erosion and deformation, they retain important structural and lithologic information on the deep central portions of large impact basins. Recent reconstructions of the Sudbury basin (e.g., Grieve et al., 1991; Roest and Pilkington, 1994) show that the location of the peak ring corresponds to a ring of gravity maxima located near the edge of the preserved sequence (corresponding to the inner portion of the original Sudbury impact basin). The Vredefort structure is heavily eroded but has a well-expressed concentric gravity pattern similar to that over the central one-third of Chicxulub but approximately 60% as large (e.g., Antoine et al., 1990; Stepto, 1990). As described by Nicolaysen (1990), the so-called collar strata seem most likely to correspond to the structural and lithological expression of the peak ring: These rocks are highly deformed and locally overturned, and they separate the deep rocks of the crystalline core from the modestly deformed rim synclinorium of the shallower Transvaal strata. A distinct ring of gravity highs, with a diameter of 60 to 70 km, is located over this sequence. Consequently at both Sudbury and Vredefort, the central peak ring is expressed as a gravity high, not a gravity low.

Intermediate rings: Delimiting the zone of deep deformation at Chicxulub. Gravity values increase abruptly and significantly between ~70 and ~105 km from the center (Plate 1 and Fig. 2); this region exhibits the steepest gravity gradients associated with the Chicxulub structure. Its distal edge defines a prominent gravity ring (Ring 3), which Hildebrand et al. (1991) and Pilkington et al. (1994) interpret as the basin rim. Such steep inward-facing gradients define a sharp boundary to the major mass deficiency in the basin center. But because the crater topography has been completely filled with platform sediments, there should only be a very small density contrast between the crater fill and the surrounding upper crustal rocks of the crater walls. Therefore it seems unlikely that the steepest gradients observed in the structure would be associated with the rim zone, a region that, in other terrestrial impact structures, is characterized by shallow inward slumping (e.g., Pilkington and Grieve, 1992).

Although the largest terrestrial basins are either heavily modified or are associated with strong regional variations that hinder precise extraction of the gravity anomalies associated with the outer portions of the basin, assessment of some smaller terrestrial craters can provide help in linking gravity gradients with basin structure. Both the 24-km-diameter Ries crater (Jung et al., 1969; Pohl et al., 1977) and the 24-km-diameter Haughton crater (Pohl et al., 1988) are well-preserved craters with distinct gravity signatures characterized by a broad depression, the edge of which marks the location of the topographic rim (Fig. 2). In both cases, there is a sharp inward steepening in gradient near the edge of the central zone of excavation and deep deformation as determined by independent techniques (e.g., for Haughton crater, see Scott and Hajnal, 1988, and Bishoff and Oskierski, 1988). Furthermore, recent gravity and

topography data for the lunar Orientale basin by the Clementine space probe (Spudis et al., 1994; Zuber et al., 1994) show that the steepest Bouguer anomalies are located over and within the Outer Rook Ring (Ring 3; Fig. 1) and not associated with the Cordilleran Ring (Ring 4; Fig. 1), the topographic rim of this multiring basin. We believe, therefore, that Rings 2 and 3 at Chicxulub would correspond to the Inner and Outer Rook Mountain Rings at Orientale (Rings 2 and 3; Fig. 1) and that the steep gradients observed between these two rings at Chicxulub could mark the outward extent of excavation and deep deformation associated with the collapsed "transient" crater.

This measurement should not be taken as a precise estimate of the "true" transient crater diameter (the diameter of the crater as measured from the preimpact surface) as used by modelers to define scaling relationships (e.g., Melosh, 1989; Chapter 7). During collapse, the transient crater walls are severely deformed, and the zone of intense deformation is broadened somewhat. This leads to an enlargement of the gradient ring associated with the boundary between the transient crater and the more distal slumped outer basin floor. We suspect that our estimate based on gravity data would be somewhat larger than the transient crater's "rim-crest" diameter; therefore, it would overestimate the apparent diameter by >25% (Melosh, 1989; p. 112). Consequently, the most appropriate estimate of the "true" transient crater diameter resulting from analysis of the gravity data would be ~105 to 160 km.

The topographic basin rim. The outermost ring at Chicxulub is a broad, discontinuous gravity feature whose crest is located at a diameter of ~260 to 300 km. This ring is most conspicuously expressed to the south of the basin center as it crosses and interrupts the southward-trending troughlike gravity low in Plate 1; B and C, and toward the east and north of the crater center. Sharpton et al. (1993, 1994a) have argued that this ring marks the modified topographic rim of the Chicxulub multiring basin. This ring is located at the edge of the broad circular gravity low associated with the Chicxulub basin; the anomaly edge corresponds approximately to the topographic rim at other terrestrial craters. We emphasize, however, that although the edge of the gravity depression is associated with the rim-crest region at many other terrestrial craters (e.g., Pilkington and Grieve, 1992), gravity data alone cannot pinpoint the rim location, particularly if, as is the case for Chicxulub, the basin is completely filled with sediments that are similar in density to the upper target sequence. The outermost ring is probably not an exterior ring (i.e., located outside the topographic rim), as observed at some large multiring basins on other planets, because it has a detectable gravity expression and because of its association with the edge of the basin's circular gravity low. Consequently, this ring corresponds to the Cordilleran Scarp at Orientale (Ring 4; Fig. 1). As discussed in a later section, this interpretation is supported by well data.

Magnetic data

The magnetic anomaly map of the Chicxulub structure, compiled from aeromagnetic surveys, is shown in Plate 1; D. An ~80-km-diameter zone of high-frequency dipolar magnetic anomalies with amplitudes of up to 1,000 nT occupies the center of the structure (as determined by concentric gravity anomaly patterns). This strongly magnetic zone is flanked by a region of lower amplitude (5 to 20 nT) high-frequency magnetic anomalies extending out to a radial distance of ~100 km. The magnetic signature of the Chicxulub structure is distinct from the regional magnetic characteristics of the attenuated continental crust of the Yucatan Peninsula. The central zone of high-amplitude magnetic anomalies is located within the first gravity ring and appears to be offset westward from the center of the gravity anomalies.

Pilkington et al. (1994) suggest that these magnetic anomalies reflect a thick sheet of impact melt rocks covering the crater floor, with the strongly magnetic central zone due to a deep central melt pool analogous, they state, with the craters Dellen and Mien. If other terrestrial craters similar to Chicxulub actually demonstrated a clear association between magnetic patterns and melt-rock distribution, then magnetic patterns would provide a reasonable constraint to crater size, as they propose. But terrestrial craters display highly variable magnetic characteristics (e.g., Pilkington and Grieve, 1992), and it is not the case that magnetic anomalies unambiguously delineate melt sheets in general. Both Mien (5-km diameter) and Dellen (15-km diameter) are impact structures on purely crystalline terrains, conducive to the formation of coherent melt sheets. On the other hand, the Chicxulub basin formed by impact into volatile-rich target rocks, and other craters into such lithological sequences rarely contain appreciable coherent melt sheets (e.g., Kieffer and Simonds, 1980). Haughton crater, for instance, has no coherent melt sheet but shows a central zone of high magnetization (Pohl et al., 1988) that is considerably smaller than the crater floor defined on the basis of surface mapping and seismic studies (Fig. 2).

Vredefort experienced such extensive erosion that, if a melt sheet was formed, it has subsequently been removed by erosion and only dikes of "bronzite granophyre" (French and Nielsen, 1990) remain as evidence of wholesale melting during impact. Nonetheless, Vredefort has magnetic anomalies that are comparable in amplitude and frequency to those observed over Chicxulub (Antoine et al., 1990; Hart et al., 1995). The magnetic highs are inboard of the uplifted, highly deformed collar strata (Antoine et al., 1990) that, as we discussed previously, seem to correspond with the central peak ring. The cause of the magnetization appears to be impact-induced thermal metamorphism of the deformed deep crustal rocks composing the central uplift (Hart et al., 1995). We therefore suggest that the principal source of the magnetization at Chicxulub could also be the highly deformed and uplifted deep crystalline basement inside the peak ring. Core samples of Chicxulub's melt rocks are strongly magnetic (Sharpton et al., 1992; Urrutia-Fucugauchi et al., 1994), and melt rock deposits may contribute to its magnetic signature. However, it is not clear whether or not there is a coherent, laterally extensive sheet of impact melt rocks within the Chicxulub basin or, if it does exist, what its dimensions are.

GENERAL STRATIGRAPHIC FRAMEWORK FROM WELL DATA

The eight wells drilled into and around the Chicxulub structure provide a stratigraphic framework that is consistent with a large impact structure formed at the K/T boundary. For core-sample locations, the convention for identifying wells is as described in the caption of Plate 1. Core intervals are preceded by an N (for *núcleo*, Spanish for core), so a complete description of the fourteenth core interval recovered from the Yucatan No. 6 well would be Y6-N14. All depths are referenced to sea level. The stratigraphic correlations derived from drill core samples and well logs are summarized in Fig. 3.

Pre-impact stratigraphy, target characteristics, and basin shape

The rocks involved in the Chicxulub impact event are silicate basement of continental affinity overlain by a shallow-water platform sequence consisting of Lower Cretaceous (or older) evaporites and younger limestones and dolomites. The wells on the flanks of the structure (Yucatan-1 and Yucatan-4) indicate between 300 and 800 m of evaporite in the platform section; however, the evaporites seem to thicken toward the center of the structure. It seems likely that outwardly directed compression during the early stages of the impact event (Croft, 1981a, b) could have structurally thickened the sequence at radial distances equivalent to Ticul-1 or even Yucatan-2, but scarcity of well data and uncertainties in the size of the structure allow other explanations as well. In any event, it seems unlikely that there is as much anhydrite as previously estimated by Lopez-Ramos (1983) who, relying upon reports based on analysis of well cuttings, mistook the anhydrite-dolomite breccia in the Upper Cretaceous section (Fig. 3) for interbedded anhydrite and dolomite layers. As we discuss below, we now recognize that this unit is debris ejected from the Chicxulub basin and deposited onto the preexisting Upper Cretaceous rocks around the impact site.

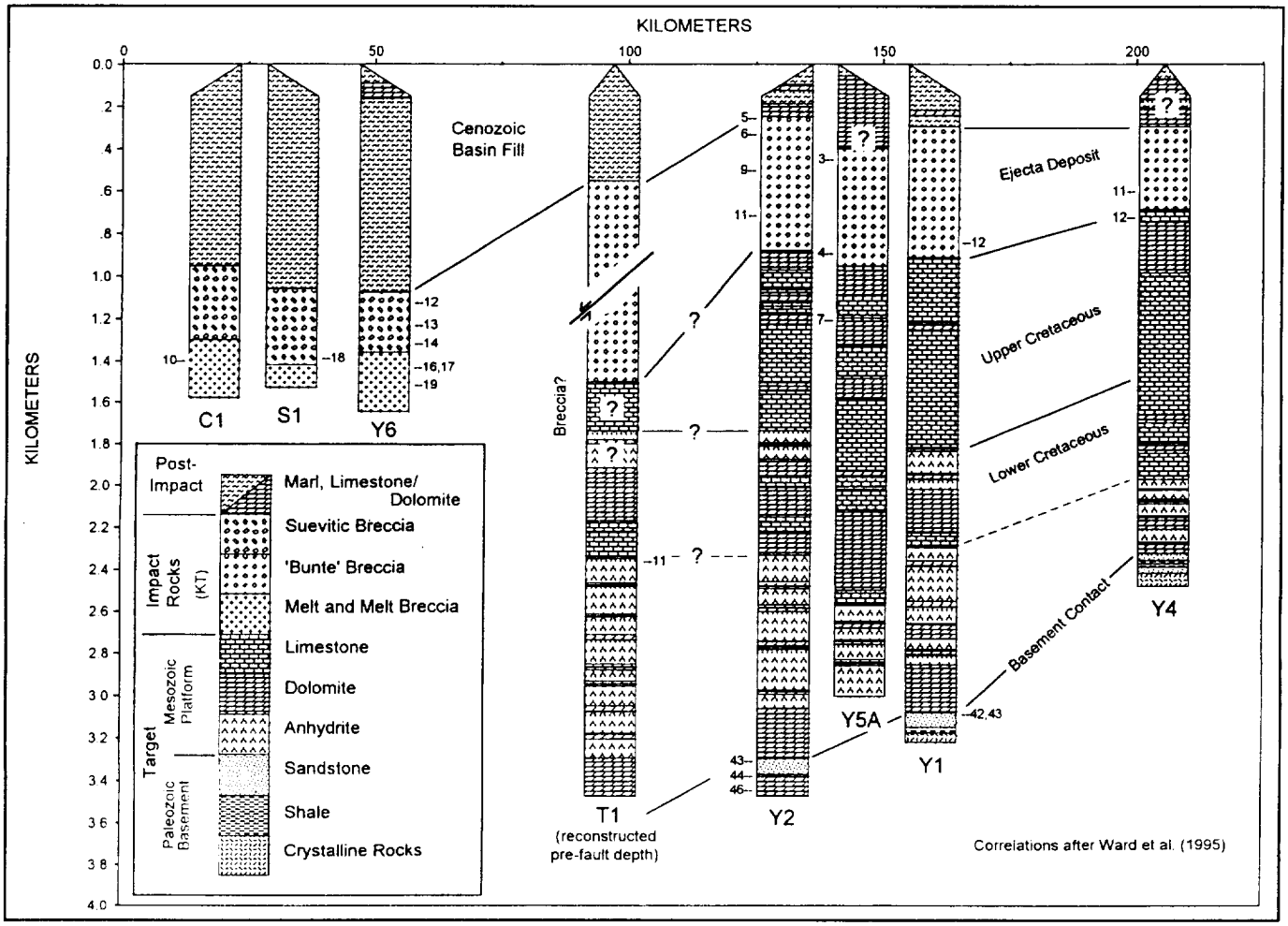

Figure 3. Stratigraphic correlations across the Chicxulub basin based on well logs and sample analysis. Wells are arranged in distance from the basin center. The samples we have studied are identified by numbers. Other lithological assignments are based on visual inspection of cores, updating previous published and unpublished reports. The stratigraphic thickness of the breccia unit in T1 reflects the pre-fault conditions we infer from analysis of well-log data and drilling reports. True (present) depths can be calculated by removing 200 m from the depths of all units below the fault shown. Major stratigraphic correlations are based on the work of Ward et al., 1995.

Based on well data alone, the Chicxulub basin extends ~135 to 150 km from center to the vicinity of Yucatan-2, Yucatan-5A, and Yucatan-1, where the K/T boundary is nearest to the present surface (Fig. 3) . This distance corresponds to the location of the fourth and outermost ring of gravity anomalies (Plate 1 and Fig. 2). Filling the basin are Tertiary limestones and marls ranging in thickness from slightly over 1 km near the center to less than 300 m at the basin rim. The total thickness of platform rocks at the time of the impact is constrained by depth to basement outside the structure (removing the thickness of the Tertiary section) and is ~2 km in Y4 as well as in several other wells located east and south of the structure between 200 and 300 km from the center, such as Quintana Roo 1, Tower Hill 1 and 2, and the Basil Jones 1 wells (Lopez-Ramos, 1983).

In wells located within ~160 km of the center, that is, Ticul-1, Yucatan-1, Yucatan-5A, and Yucatan-2, the silicate basement appears to be 750 to 1,000 m deeper than in more distant wells (Fig. 3). This is consistent with faulting and sagging associated with downward collapse and widening of the basin that occurs during the final modification stage of the impact process (Croft, 1981 b). The deepening of the basement contact in wells within the Chicxulub basin appears to be too abrupt to be explained solely by a regional basement tilt as previously proposed (e.g., Viniegra, 1981): Yucatan-5A is less than 70 km west of Yucatan-4, yet reached total depth of 3,003 m still in platform rocks whereas the basement contact at Yucatan-4 was reached at ~2350 m—at least 650 m higher. Outcrop patterns in northern Yucatan (Plate 1; A) indicate a modest northward-trending epirogenic rise located slightly west of the peninsula's center, suggesting that Cenozoic units on the eastern side of the basin tilt gently to the east, not west. There are also no indications of significant westward regional tilting of the pre-Cenozoic units in offshore seismic profiles located ~40 km north of the basin center (Camargo Z. and Suárez R., 1994). Nor are there indications of basement contacts as deep as those around the Chicxulub basin in any of eight onshore wells drilled between 160 and 450 km of the center of Chicxulub (Lopez-Ramos, 1983).

The Upper Cretaceous–Lower Cretaceous contact is also substantially deeper in wells inside the basin (Fig. 3), consistent with downward (and inward) displacement of the pre-Cenozoic crustal column during collapse of the transient crater (e.g., Melosh, 1989). We believe, therefore, that these vertical offsets, which could exceed 1 km, reflect structural displacements induced during the collapse (modification) stage of this impact event. These observations support the interpretation that the outermost gravity ring, located ~140 km from the center of Chicxulub, marks the topographic basin rim (Sharpton et al., 1993).

Impact lithologies

Foremost in support of the impact origin of the Chicxulub structure is a lithological sequence similar to that observed at several other large well-studied terrestrial impact structures such as the Ries crater (von Engelhardt, 1972; Hörz et al., 1983), Haughton crater (Redeker and Stöffler, 1988), and the Popigai structure (Masaitis et al., 1980; Masaitis, 1990). Elements of this characteristic rock assemblage are also observed at other more eroded impact structures, such as the Sudbury structure. The sequence consists of suevitic breccias, weakly shocked crater fill and ejecta deposits equivalent to the Bunte Breccia at the Ries crater, melt rocks, and melt-matrix breccias.

The Chicxulub suevite breccia. Three Pemex exploratory wells are located near the center of the concentric gravity anomalies over the Chicxulub structure (Plate 1) and all intercepted breccias and crystalline silicate melt rocks at depths of ~1 km below sea level (e.g., Lopez-Ramos, 1983). Core samples from the Y6 and S1 include suevite (Plate 2; A-C), a polymict, clastic-matrix breccia containing impact-generated glass and melt-rock clasts analogous to impact-produced breccias observed at several other terrestrial craters such as Ries (e.g., Stöffler et al., 1977), Wanapitei (Dressler, 1982; Grieve and Ber, 1994), and Haughton (Redeker and Stöffler, 1988). Suevite characteristically contains deformed clasts of melt rock and glass. Like these other crater suevite units, the suevite deposits within Chicxulub are predominantly composed of highly shocked rocks from the lower parts of the target stratigraphy and contain abundant glass and deformed melt clasts (Sharpton et al., 1992).

The Chicxulub suevite recovered from the Pemex wells seems to be graded, ranging from sand-sized clasts near the top (Y6-N13; 1,100 to 1,103 m) to pebble-sized clasts at Y6-N14 (1,208 to 1,211 m) and S1-N18 (1,365 to 1,368 m) (Plate 2; A-C). This grading indicates that the breccia sequence most likely represents fall-back ejecta that was either sorted during transport through the atmosphere or ocean or subsequently reworked. At the Ries crater, sorted suevite is also observed but only near the top of the suevite sequence (Stöffler, 1977; Newsom et al., 1990), suggesting the possibility that the Chicxulub suevite deposits may extend much deeper than the current drill cores reach.

Pilkington et al. (1994) envisage the peak ring of the Chicxulub impact crater as a thick wedge of this upper breccia floating on a thick pool of impact melt rock. In addition to the problems with this interpretation discussed earlier, the evidence that these upper breccias are normally graded, and thus reworked, provides further evidence that they are unrelated to a primary element of crater morphology like the central peak ring.

Constraints on biostratigraphy and paleoenvironment. The carbonate unit recovered from Y6-N12 (1,000 to 1,003 m) immediately above the suevite contains a well-preserved fossil assemblage consisting mainly of abundant planktic foraminifera of the genera *Globigerina* and *Globorotalia*. The following age-significant species were identified (Marín et al., 1994): *Globorotalia pseudobulloides*, *Globorotalia trinidadensis*, and *Globigerina triloculinoides*. Each of these forms has the base of its stratigraphic range in the lower Danian; consequently, the carbonates containing these fossils are Paleocene and not Upper Cretaceous as previously suspected (Lopez-Ramos, 1983). The Y6-N13 suevite sample (Plate 2; A) contains no for-

ams younger than latest Maastrichtian, consistent with a K/T age for the Chicxulub-forming impact event.

The fossil assemblage within the suevite samples Y6-N13 and N14 (Plate 2; A, B, F, G) includes orbitoid foraminiferids, mollusk fragments, and algal fragments. This shallow-water assemblage indicates that water depths prior to the impact event were at most a few tens of meters. By the time the Y6-N12 interval was deposited (Lower Danian), the water depth in this portion of the basin (Plate 1; A) was considerably deeper, based on the abundant occurrences of planktonic forams in general. Frequent occurrences of *Globorotalias* suggest an outer neritic environment (approaching 200-m water depths) or beyond. A single occurrence of *Nuttallides* implies an upper bathyal environment. Based on our evaluation of the stratigraphic correlations from well data (Fig. 3), relief across the basin during Lower Danian was ~700 to 800 m.

Characteristics of the silicate basement as revealed in suevite samples. Centimeter-sized fragments of fine- to coarse-grained silicate basement are common in Y6-N14 and S1-N18 breccias and indicate a medium- to high-grade metamorphic terrain. The predominant basement rock is pink, medium- to coarse-grained granitic gneiss (Plate 2; H-L) containing 10 to 20% quartz, 60 to 80% alkali feldspar, and 10 to 20% low-calcium plagioclase. The results of an electron microprobe survey of feldspar grains from Y6-N14 are summarized on the ternary diagram shown in Figure 4. Minerals such as biotite, pyroxene, or hornblende are rare in the granitic clasts, most likely because of their greater susceptibility to postshock alteration and their lower melting temperature. Sphene, apatite, and zircon exist as trace minerals. Grain boundary relationships within these fragments reveal substantial shearing and recrystallization before impact. In addition, ~20% of the phyllosilicate clasts in Y6-N14 contain ≤1-mm-wide irregular domains of relict glasses (Plate 2; R) (Sharpton et al., 1992) that are similar in major element chemistry to feldspars in the granitic clasts; however, microprobe analyses of these glasses consistently yield low totals (~91 wt%), suggesting that they have incurred secondary hydration associated with diagenesis. In conjunction with the unmelted granitic clasts observed in Y6-N19 melt-rock samples, these mineral glasses demonstrate that granitic gneiss is a major constituent of Chicxulub melts. Other basement clasts include quartz-mica schist, metaquartzite, and rare occurrences of mylonite. These rock types are similar, in terms of their mineralogy, structural fabric, and texture, to the shocked lithic clasts distributed within the K/T boundary (Sharpton et al., 1990a, b; Izett, 1990).

Evidence of shock metamorphism. The suevite unit intercepted by wells Yucatan-6 and Sacapuc-1 (Plate 1 and Fig. 3) contains clasts of silicate basement and platform rocks showing abundant and unequivocal evidence of shock metamorphism including: (1) planar deformation features in quartz, feldspar (Sharpton et al., 1992), and zircons (Krogh et al., 1993) (Plate 2; F-L), indicating dynamic pressures up to 23 GPa; (2) shock mosaicism in quartz and feldspar grains; (3) diaplectic glasses (i.e., glasses produced from mineral clasts by the destruction of crystal order during shock compression but without fusion) from quartz and feldspar (maskelynite), which record peak pressures in the range of 30–45 Gpa; (4) fused mineral glasses, particularly of alkali feldspar, indicating shock pressures above 45 Gpa (Plate 2; R); and (5) whole rock melts (>60 GPa). Examples of these features found in various Chicxulub samples are shown in Plate 2 (F-R).

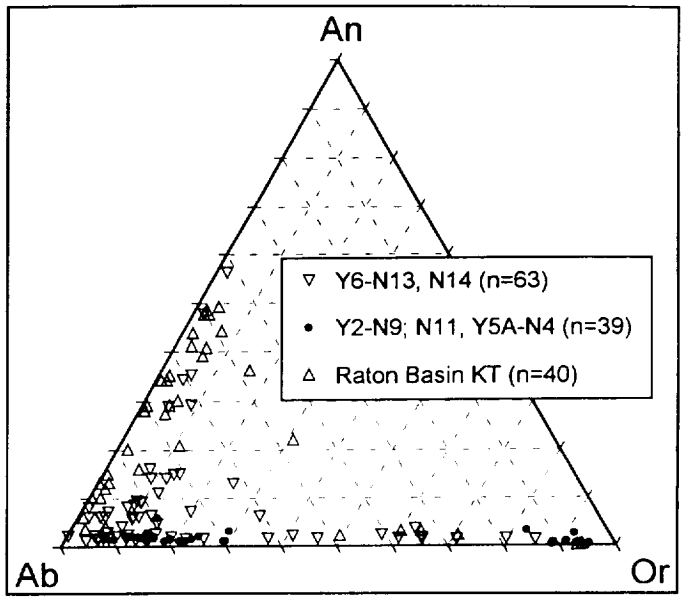

Figure 4. Feldspar cation compositions plotted on Anorthite-Albite-Orthoclase (An-Ab-Or) ($CaAl_2Si_2O_8$-$NaAlSi_3O_8$-$KA1Si_3O_8$) ternary diagram. This diagram shows the similarity between shocked feldspar grains extracted from the K/T boundary layer in Raton, New Mexico, and those from the central suevite (Y6 samples) and the distal Bunte Breccia–type deposits of Yucatan-2 and Yucatan-5A.

Melt rocks and melt matrix breccias. Below the deposits of suevite (Fig. 3) are occurrences of impact melt and melt-matrix breccia (Plate 2; D, E, Q) showing ubiquitous evidence of chemical and thermal disequilibrium and superheating as is characteristic of impact melt rocks. Melt-rock textures of the various core intervals are distinctly different (Plate 2), most notably in the size and abundance of undigested clasts, variations in color, grain size, and porosity of the matrix and in evidence of alteration. Brief descriptions of these melt rocks follow. For more information see Schuraytz et al. (1994).

The C1-N10 sample (Plate 2; E, S) is distinct from Y6 samples with respect to both the virtual absence of unmelted clasts and the coarser grain size of the matrix. The matrix is dominated by an intersertal arrangement of subhedral to euhedral pyroxene (augite) up to 0.7 mm in length and plagioclase (andesine to labradorite) showing a range of crystal morphologies and ranging up to 1 mm in length. The mesostasis of C1-N10 includes alkali feldspar and plagioclase ranging from oligoclase to pure albite.

Approximately 35% of Y6-N17 is undigested silicate basement clasts. These clasts show a bimodal size distribution dominated by single mineral fragments and polycrystalline domains

of highly deformed, recrystallized quartz and feldspar ranging from <1 mm up to ~4 mm in length. Subhedral augitic pyroxene prisms (10 to 70 μm long) form coronas surrounding quartz clasts and pervade the interiors of more highly disrupted granitic domains, with aggregates up to 1 mm. The primary constituents of the matrix are subhedral to euhedral microphenocrysts of augite and plagioclase ranging from 5 to 15 μm in length. These are set in a porous, cryptocrystalline mesostasis containing albite, quartz and potassium feldspar. Anhydrite and gypsum constitute ~8% of total rock volume in the thin sections we have studied, mostly as veins and cavity fillings, but also as clasts.

Samples of Y6-N19 (Plate 2; D) reveal a melt matrix breccia containing 2- to 11-cm-wide, angular-to-subrounded melt clasts of varied textures. The dominant melt clast type is very similar to the surrounding matrix, and in some cases the boundary between them is difficult to discern. This material is also essentially similar to Y6-N17, consisting of 5- to 15-μm-long, subhedral-to-euhedral pyroxene and plagioclase in a cryptocrystalline quartzofeldspathic mesostasis showing variable porosity. In contrast to Y6-N17, however, undigested silicate basement clasts in Y6-N19 are typically larger and show clear evidence of shock metamorphism (Plate 2; D).

Evidence of shock metamorphism in the Chicxulub melt rocks. Undigested basement clasts retain indications of shock metamorphism (Plate 2; M) but are often overprinted with subsequent thermal effects such as recrystallization and annealing.

A recrystallization effect commonly associated with shock-deformed quartz clasts observed in the Chicxulub melt rocks is the occurrence of "ballen structures" characterized by distinctive perliticlike fracture patterns that define individual optical domains (Plate 2; N). Similar features have been observed at the Ries crater (Engelhardt, 1972), Lappäjavi crater (Carstens, 1975; Bischoff and Stöffler, 1981), and West Clearwater Lake structure (McIntyre, 1968; Phinney et al., 1978). These ballen structures seem to document the strain associated with devitrification of either an impact-fused quartz glass known as lechatelierite (Carstens, 1975), or diaplectic (shock-vitrified without fusion) quartz glass (Bishoff and Stöffler, 1981). Stöffler and Langenhorst (1994) have shown that diaplectic glass displays a higher degree of long-range order than normal fused glasses quenched from a melt (e.g., silicic volcanic glasses) and effectively retains a "memory" of its previously crystalline state. Consequently, they note, diaplectic glass reverts to α-quartz + cristobalite during annealing, instead of just cristobalite as is the case with fused silica glass. Bischoff and Stöffler (1981) suggested that ballen structures record a range of peak shock pressures; those in which the ballens have different optical orientations, such as observed in the Chicxulub melt rocks, record shock pressures between 45 GPa and 55 GPa.

Target affinity and meteoritic contamination. Except for anomalous Ir enrichments in several specimens attributed to nonuniform dissemination of the projectile (Sharpton et al., 1992; Schuraytz and Sharpton, 1994), our analyses suggest that the melts were derived exclusively from continental crust and platform sediment target lithologies, with no evidence of a significant mantle or oceanic crustal signature. These results are supported by Sr, Nd, O, and Os-Re isotopic studies on the C1-N10 samples with regard to both the continental affinity of the target rocks (Blum et al., 1993) and the heterogeneous distribution of up to 3% meteoritic contamination (Sharpton et al., 1992; Schuraytz and Sharpton, 1994; Koeberl et al., 1994). Considering current constraints on excavation depth (15 to 25 km) of the Chicxulub impact event (Sharpton et al., 1994b) and the potential lithologic diversity within this volume, the observed chemical variability (andesitic to dacitic) is rather small and in keeping with the gross compositional homogeneity of melt rocks from other terrestrial impact structures, such as Manicouagan (Grieve and Floran, 1978) and West Clearwater (Simonds et al., 1978). However, given that Chicxulub melt compositions were derived from very small samples compared to those available from other well-exposed melt sheets, some heterogeneity might be expected. Furthermore, because currently available Chicxulub specimens represent an inordinately small sampling of the upper ~100 m of known melt rock, the limited compositional range should be regarded as tentative, as should comparisons with smaller structures where the upper part of the melt sequence has been eroded. Finally, all samples from Chicxulub have been modified to some degree by hydrothermal alteration (Schuraytz et al., 1994).

Are these rocks from a coherent melt sheet? Several workers have interpreted these melt rocks as the Chicxulub melt sheet (Hildebrand et al., 1991; Pilkington et al., 1994), however, the current constraints on lateral and vertical continuity of these melt zones are very poor and it seems premature to interpret these deposits as necessarily representative of a coherent melt sheet. Isolated melt zones are observed in the Sudbury structure associated with the fall back sequence (Onaping Formation); similar "stratiform melt bodies," several tens to a few hundred meters thick have been documented within the suevite breccias from the 100-km-diameter Popigai structure (Masaitis et al., 1980; Masaitis, 1990) and the 45-km-diameter Montagnais (Jansa et al., 1989, 1990). Furthermore, some large impact basins—Montagnais, Popigai, and Kara (Masaitis et al., 1980), for instance—show no evidence of the thick, laterally continuous melt sheets observed at others such as Manicouagan and Mistastin. Observations that suggest the melt rocks from Chicxulub represent local pods of melt, possibly within a thick suevite unit, rather than a thick coherent melt sheet include (1) the typically fine grain size of the melt matrix, (2) the clast-rich nature of the melt, including the presence of xenocrysts of anhydrite and carbonate rocks, (3) the presence of diaplectic glasses, (4) the chemical variability in the melt rock assemblage (Table 1 in Schuraytz et al., 1994), and (5) the nonuniform distribution of siderophile elements within the melt rocks. Consequently, a coherent melt sheet at Chicxulub, if it exists at all, may reside at considerably greater depth than any drilling to date has reached.

The Chicxulub multiring basin and the K/T boundary. Melt rocks within the Chicxulub crater have experienced varying levels of hydrothermal alteration and albitization (Sharpton

et al., 1992; Schuraytz and Sharpton, 1993; Schuraytz et al., 1994); however ^{40}Ar-^{39}Ar determinations on relatively pristine melt-rock samples from the center of the basin indicate a crystallization age of 65.0 ± 0.4 Ma (Sharpton et al., 1992) or 64.98 ± 0.05 Ma (Swisher et al., 1992) which is at or very near the K/T boundary. Evaluation of the magnetization of these and other samples shows that they cooled during an episode of reversed geomagnetic polarity, consistent with a K/T boundary age (Sharpton et al., 1992; Urrutia-Fucugauchi et al., 1994).

Analysis of the Rb-Sr, O, and Nd-Sm isotopic systems confirms a chemical link between the Chicxulub melt rocks and the impact glasses contained in the K/T boundary unit at Beloc, Haiti (Blum et al., 1993); the Beloc tektite-bearing unit appears to be equivalent to the lower, kaolinite-rich member of the K/T boundary couplet in the Western Interior. Krogh et al. (1993) recently determined U-Pb ages of zircon xenocrysts from Chicxulub breccia sample Y6-N13 to be ~545 Ma, with a small percentage showing a 418-Ma age. The population of 545-Ma zircons matches the crystallization age of zircons extracted from the upper member (magic layer, fireball layer, etc.) of the K/T doublet in western North America, and both ~545-Ma and 418-Ma zircons have been detected in the tektite-rich K/T boundary layer at Beloc (Krogh et al., 1993; Kamo and Krogh, 1995). Unmelted breccia clasts, representing the silicate basement involved in the Chicxulub basin-forming event, are medium- to high-grade continental crust (Plate 2; H-L) similar to the lithic clasts observed within K/T boundary sediments from around the world (Bohor et al., 1984, Bohor, 1990; Izett, 1990; Sharpton et al., 1990a, b; 1992; 1994a). For instance, Figure 4 shows the match between feldspar compositions of shocked basement clasts within Chicxulub suevites and ejecta deposits with shocked feldspars from the upper member of Raton Basin K/T boundary layer. These observations provide compelling evidence that the Chicxulub impact event is responsible for both the shocked minerals observed in the upper member of the K/T boundary sequence and the glass-rich lower member. Consequently all evidence to date points to a singular, extremely energetic, and deadly impact event at the K/T boundary.

Ejecta and allogenic impact breccia deposits (Bunte Breccia equivalents). The central portion of the Chicxulub basin, showing high-amplitude magnetic and gravity anomalies and deeply buried occurrences of suevite breccias and melt rocks, is flanked by a broad annular trough, extending outward to ~150 km from center, where the pre-Tertiary sequence is depressed by up to 1 km. Filling this trough and covering outlying areas is a breccia sequence consisting of centimeter-scale clasts of dolomite, limestone, and anhydrite in a clayey-micritic matrix. This unit was completely overlooked by Lopez-Ramos (1983), who compiled his lithostratigraphic data for the Chicxulub region primarily from analyses of drill cuttings. Marshall (1974) was the first to document this "clastic anhydrite-dolomite lithofacies" and Hildebrand et al. (1991) first reported evidence of shock-deformed quartz clasts within sample Y2-N6 near the top of this sequence. However, Hildebrand et al. (1991) did not interpret the entire breccia sequence as Chicxulub ejecta. Instead they envisaged only a "90-m thick ejecta horizon," with the Y2-N6 sample representing the base of this unit. The ejecta thickness at the Yucatan-2 well site has been a fundamental line of evidence used for the 170-km estimate of Chicxulub's diameter (Hildebrand et al., 1991; Hildebrand, 1992, 1993; Kring, 1993; Pilkington et al., 1994). We now have compelling evidence, however, that the whole anhydrite-dolomite–bearing breccia unit is the continuous ejecta deposit at Chicxulub as independently proposed by Pope et al. (1993) and Sharpton et al. (1994a, b).

We have found trace quantities (<1% volume) of shocked but unmelted silicate basement clasts and melt-rock clasts with small xenocrysts of shocked quartz and feldspar (Plate 2; O-Q) in all our samples throughout the anhydrite-dolomite breccia shown in Figure 3. Shocked feldspar crystals within larger melt clasts have compositions similar to those found within the Chicxulub suevite breccias and the K/T boundary layer (Figure 4). This evidence demonstrates that the anhydrite-dolomite breccia unit is the Chicxulub crater's continuous ejecta deposit and is analogous to the well-studied Bunte Breccia at the Ries Crater (Hörz and Banholzer, 1980; Hörz et al., 1983). It is likely that the proportion of silicate basement apparent in these breccia samples has been diminished by the effects of chemical alteration and secondary mineralization working on the highly vulnerable shocked and partially melted basement clasts. At the Yucatan-2 well site (where this unit previously was estimated to be ≤90 m thick), this unit is >600 m thick, and the top of the unit is located ~250 m below sea level.

Pilkington et al. (1994) noted that published reports do not show an Upper Cretaceous breccia unit occurring at the Ticul-1 well (~95 km from center) and claim that this provides strong evidence that Chicxulub cannot be a 300-km-class impact basin. However, with the exception of the work conducted at the University of New Orleans (Marshall, 1974; Weidie et al., 1978; Ward et al., 1985; Weidie, 1985), this breccia was not recognized in *any* wells; Lopez-Ramos (1983) shows a sequence of interbedded anhydrite and carbonate units in the uppermost Cretaceous section in Yucatan-1, Yucatan-2, Yucatan-4, and Yucatan-5A at stratigraphic levels where breccia was subsequently reported by Marshall (1974) and Weidie et al. (1978). This circumstance was primarily due to the fact that the University of New Orleans (UNO) group focused on core studies, whereas previous reports were based predominantly on analyses of drill cuttings. Ticul-1 core samples were not available to the UNO group, so it is not surprising that the breccia was not recognized there.

Several lines of evidence indicate that the Upper Cretaceous section at Ticul-1 is indeed predominantly, if not totally, composed of anhydrite-dolomite impact breccia. Well reports show the K/T boundary at Ticul-1 to be located at 550 m, and the Upper Cretaceous section down to at least 1,200 m consists of interbedded evaporites, marls, limestone, and dolomite with signs of reworking. These well-cutting descriptions are similar

to the descriptions of the Upper Cretaceous unit at Yucatan-2, Yucatan-1, Yucatan-4, and Yucatan-5A that is now recognized to be impact breccia. Furthermore, the only primary (bedded) anhydrites recovered in drill cores in northern Yucatan are located in the Lower Cretaceous section. Therefore, occurrences of Upper Cretaceous anhydrite at Ticul-1, where the section is located at greater depth than at Yucatan-2, Yucatan-5A, and Yucatan-1, most likely signify breccia containing Lower Cretaceous anhydrite excavated during impact.

Ward et al. (1995) have conducted detailed stratigraphic analysis of the wells in the vicinity of Chicxulub based on well logs, biostratigraphy, and lithostratigraphy of existing samples. They find the pre-Cenozoic section in the Ticul-1 well to be 200 to 300 m shallower than similar strata at the Yucatan-2 well. We attribute this to the intersection of the Ticul-1 core with the northward-dipping normal fault system shown in Plate 1 (Ticul Fault). This is consistent with the present topography across the scarp, which constrains the vertical offset on the fault to be in excess of ~100 m. Ward et al. (1995) show this fault intersecting the core at ~1-km depth, still within the zone where Pemex well reports show evidence of impact breccias. Consequently, more than 200 m of the original breccia thickness have been removed by normal faulting, and we infer a conservative lower bound of 900 m for the ejecta thickness at Ticul-1. Well logs and coring efforts provide some indications that it might be considerably thicker.

No coring was undertaken at Ticul-1 in the section above 1 km. However, 10 1-m core intervals were attempted in the Cretaceous section between depths of 1,150.8 and 2,137.7 m, but recovery was minimal, averaging less than 5%. The recovered fragments from these core tests were primarily anhydrite clasts that ranged in size between 2 and 10 cm. This poor recovery indicates a highly friable anhydrite-bearing material at these depths, possibly a reworked allogenic breccia deposit or shattered target rocks. Visual inspection of existing core samples taken from greater depths and dip-meter data show these rocks to be anhydrite blocks with considerable variation in the attitudes of bedding; these blocks are pervaded by thin veins of breccia consisting of anhydrite and dolomite clasts in a dolomitic mudstone matrix (e.g., T1-N11; 2,177 to 2,182 m; 100% recovery). This sequence could represent the original evaporite-rich platform target disrupted by ejecta emplacement and other impact processes.

Because there is no evidence of Upper Cretaceous bedded evaporites, anhydrite clasts may provide a lower constraint on the proportion of "primary ejecta" mixed with local material in this deposit. At Yucatan-2, anhydrite clasts (Plate 2; T), averaging ~0.5 mm to ~3 cm in length, account for 10 to 20% of the total volume in samples we have analyzed. If, as the well logs suggest, bedded anhydrite constitutes no more than about one-third of the total pre-Tertiary platform sequence, then the breccia at Yucatan-2 is at least 30 to 60% primary ejecta. Based on analyses of ejecta deposits at the Ries crater, such an enrichment is expected only very near the final basin rim of large impact structures (Hörz et al., 1983).

A STRUCTURAL MODEL OF THE CHICXULUB IMPACT BASIN

A structural model of the Chicxulub basin based on the evidence presented above is shown in Figure 5. Although there are still many unknown and poorly constrained aspects to this buried basin, we suggest that this model is more consistent with current knowledge of this structure and the cratering process than is the model proposed by Hildebrand et al. (1991) and Pilkington et al. (1994). The model of Pope et al. (1993) is in good agreement with our own interpretation of the location of the topographic rim. In that model, the center of the cenote ring (Plate 1A) defines the basin center (located east of the center based on gravity anomalies) and that offset results in the slightly lower basin size estimate of 240-km diameter rather than the ~260- to 300-km diameter we derive from our gravity analysis. However, given the lack of well data and gravity stations in the offshore western part of the basin as well as uncertainties associated with the cenote ring, either estimate is permitted. Evaluation and refinement of these models are possible through acquisition of high-quality seismic data across the Chicxulub basin, additional gravity data for the western portion of the basin, and a program of deep and shallow drilling within and around the basin.

Analysis of the ejecta deposits surrounding the Ries crater indicates that approximately 30% of the Bunte Breccia represents "primary" material derived from within the excavation cavity, the rest being local materials incorporated into the breccia during its energetic emplacement (Hörz et al., 1983). Accepting this estimate for Chicxulub and assuming the average thickness of the Chicxulub ejecta is 400 m, there would be more than 20,000 km^3 of primary ejecta located between 135 and 300 km from center around the Chicxulub structure. Because this breccia unit is derived predominantly from the 2 to 2.5-km-thick sequence of Mesozoic platform rocks, the excavation cavity would have to be at least 110 km in diameter just to account for the breccia deposited within that range. Additional ejected materials deposited inside or beyond this zone as well as the platform rocks that were melted or vaporized would increase this estimate, as would any additional ejecta that has been removed by erosion.

The conservative lower constraint on transient crater "true" size (>110 km) presented herein, therefore, is in reasonable agreement with the 130 ± 25-km-diameter estimate based on our analysis of gravity data. The Schmidt-Holsapple crater scaling relationship, derived primarily from theoretical and laboratory-scale constraints (Schmidt and Housen, 1987), indicates that such a crater could be generated by a 15-km-diameter comet (ρ = 1,100 kg m^3) striking the Yucatan Platform at 57 km s^{-1} (corresponding to the mean impact velocity of a long-period comet; Weissman, 1982). This object's size is somewhat

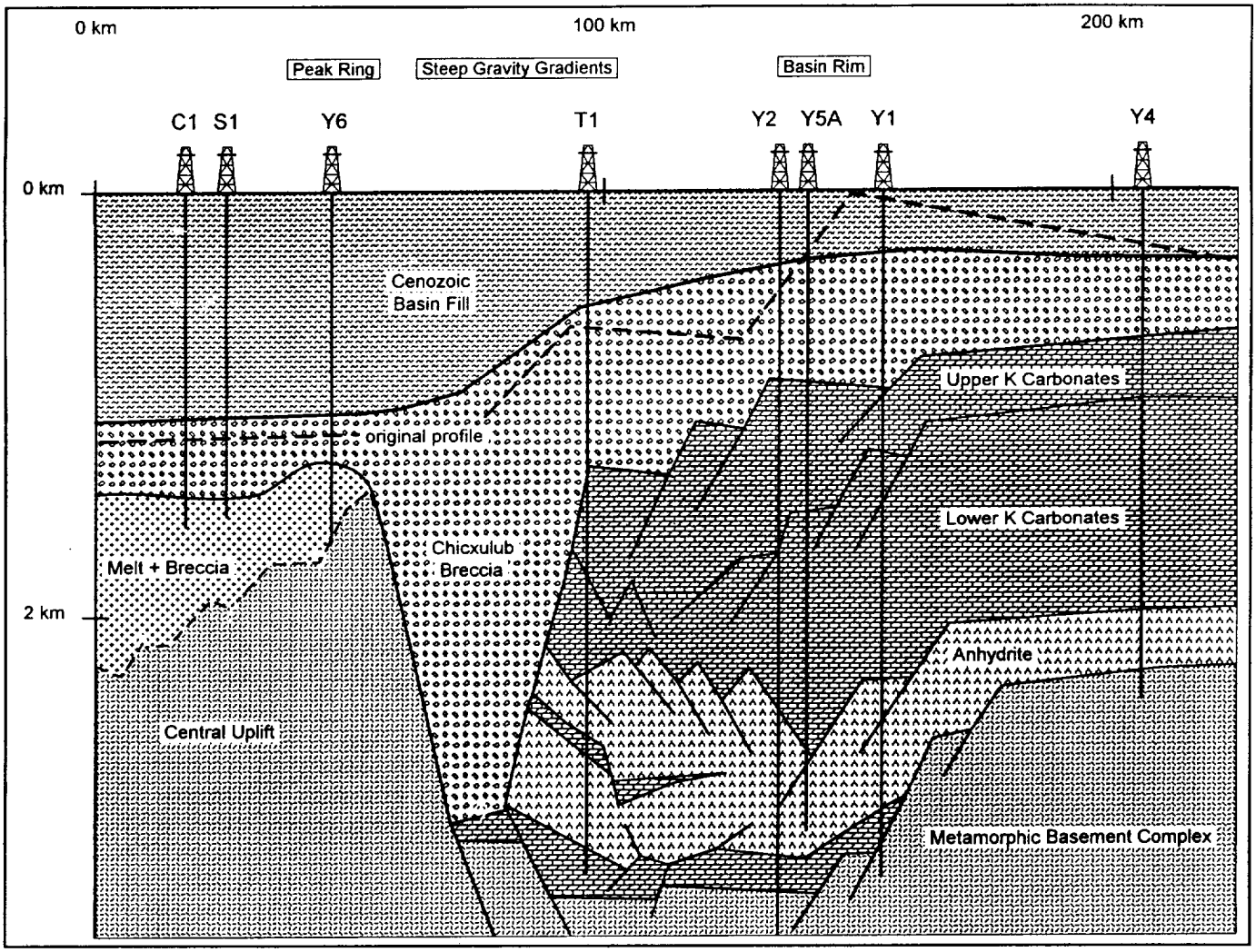

Figure 5. Schematic model of the Chicxulub impact basin that we derive from the analysis in this chapter. This simplified cross section shows the generalized present-day configuration of the crater consistent with geophysical data and well information. Erosion at the time of impact could rearrange the upper crater units significantly and reduce crater topography. Original profile shown as dashed line is reconstructed from the generalized topographic profile of the 270-km Mead Basin on Venus (Fig. 6).

larger than the canonical 10-km-diameter chondritic asteroid proposed by Alvarez et al. (1980) from their estimate of the amount of iridium distributed worldwide at the K/T boundary. However, recent analysis of the population of potential Earth-striking objects indicates that craters greater than 100 km in diameter are approximately five times more likely to have been produced by comets than by asteroids (Shoemaker et al., 1990). If the object were a comet, chondritic material might represent only a small proportion (<10% to 50%) of its total mass, the rest being ices, carbon, and other volatile components.

A 15-km-diameter comet containing 30 wt% chondritic material could account for the estimated iridium distributed worldwide at the K/T boundary (~2.5×10^{11} kg Ir) if all Ir were partitioned into the boundary layer. But, as we have shown, some projectile remains in the melt rocks deposited within the Chicxulub impact basin, and particularly at cometary impact velocities, there is a reasonable likelihood that some was expelled from the Earth (Vickery and Melosh, 1990). Given the above, we suspect that the K/T event was generated by an ~15-km-diameter long-period comet. However, because the integrated iridium mass within the K/T boundary only provides a lower constraint on the size of the impacting body, larger, more energetic objects cannot be ruled out.

We suspect that the best planetary analog to Chicxulub is the 270 km Mead basin on Venus (Fig. 6); altimetry from the Magellan mission indicates that the rim of this feature rises 300 to 400 m above the surrounding plains (Fig. 5). Because the sea covering the Yucatan platform would most likely have

been less than 50 m deep prior to impact, the rim deposits and much of the ejecta blanket must have stood above sea level and exposed to erosion, even if the crater is significantly smaller than we estimate. Consequently, the crater shape has been substantially modified from that of a pristine impact basin. Whatever remnants of the original outer crater walls survived the water-laden impact event itself would be reworked quickly in the tidal environment of the Yucatan platform. The preserved portions of the rim and ejecta units therefore represent minimum thicknesses. This suggests that ejecta deposits at the rim, that is, near Yucatan-2 or Yucatan-5A, may have been ~1 km thick prior to erosion and redistribution.

At the Ries crater, which exhibits the best preservation state of a complex crater's ejecta deposits, the weakly shocked, shallow-sourced Bunte Breccia is overlain by suevitic ejecta containing considerably more deep-seated basement clasts and exhibiting a higher degree of shock deformation. Similar breccia units have not been reported from around the Chicxulub crater, possibly because they have been eroded from the high-standing rim zone. We would expect to find these deposits, however, just inside the topographic rim (equivalent to the "megablock zone" at Ries) where such suevitic ejecta would be deposited below sea level and most likely to be preserved.

Well data indicate a smaller proportion of the anhydrite within the Mesozoic platform sequence involved in the Chicxulub basin–forming event than previously reported (Lopez-Ramos, 1983). Consequently, the contribution of vaporized sulfate-bearing lithologies to the killing potential of this impact event requires reevaluation, particularly if the impact crater is as small as 170 to 180 km in diameter (Hildebrand et al., 1991; Pilkington et al., 1994). We suggest that vaporization of carbonates in addition to sulfates played a role in the environmental collapse. An early transient period of global cooling prompted by sulfur aerosols could be followed by a longer-lasting period of global warming resulting from enhanced concentrations of CO_2 in the atmosphere. The extreme temperature excursions produced by such a dipolar temperature shift could provoke enhanced stresses in the biosphere, giving rise to the K/T extinctions.

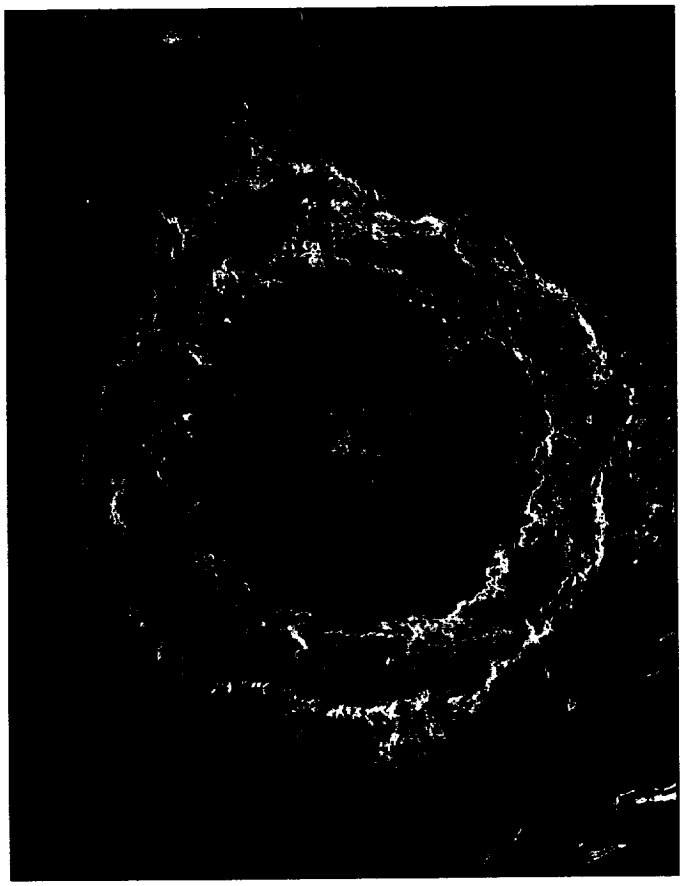

Figure 6. East-looking Magellan radar image of the Mead impact basin, the largest exposed impact structure on Venus (270-km diameter). This multiring basin is located at 12.5°N; 57.0°E. Mead may be the best planetary analog of the buried Chicxulub basin. The rim to floor depth of this feature is ~1,100 m. The outer ring is the topographic basin rim and corresponds to Ring 4 in our Chicxulub gravity model. The rim stands 300 to 400 m above the surrounding plains. Between the rim and the next prominent ring is a broad flat shelf that on average is ~350 m below the surrounding plains (~700 m below the maximum rim height). The inner scarplike ring (corresponding to Ring 3 in our model) marks a sharp drop in elevation of ~350 m to the crater center. The two innermost rings are covered by impact deposits. North is toward the top of the page.

Plate 1. **A**, Surface geology, ring locations from gravity data, and wells in the vicinity of the Chicxulub multiring impact basin. The three wells that penetrated impact melt rocks and breccias beneath the carbonate cover rocks are C1 (Chicxulub 1), S1 (Sacapuc 1), and Y6 (Yucatan 6). Other well sites shown are Yucatan 1 (Y1), Yucatan 2 (Y2), Yucatan 5A (Y5A), and Ticul 1 (T1). The Yucatan 4 (Y4) well site is located off the map, ~65 km east of Y5A. Carbonate units at the surface are Q (Quaternary; <2 Ma), Tu (Upper Tertiary; ~1.6 to 38 Ma), To (Oligocene; ~25 to 38 Ma), Te (Eocene; ~38 to ~55 Ma), and Tpal (Paleocene; ~55 to 66.0 Ma). Hatchured lines represent the Ticul fault system. Dashed lines indicate trends of ringlike zones of cenotes or sinkholes. **B,** Relief-shaded gravity anomaly data for the Yucatan region between 18° to 23°N latitude and 92° to 88°W longitude. Colors are ordered spectrally with violet and deep blue representing lowest gravity values and red representing the highest. Linear elements present in offshore data are shiptrack artifacts. Data were shaded using a low illumination angle from the north to emphasize broad low-amplitude anomalies. All data have been Bouguer corrected using a model slab density $\rho = 2{,}200$ kg m^{-3}. **C,** Relief-shaded gravity anomaly data for the Chicxulub region shown in A and D. Color coding is the same as in the regional gravity map B. Gravity anomalies in this region range from −16.4 mgal to 53.6 mgal. **D,** Aeromagnetic data for the region shown in A and C. Blues and greens represent negative anomalies; reds and yellows are positive. Data were acquired from a flight elevation of 500 m. Anomaly amplitudes exceed 900 nT near the center of the crater.

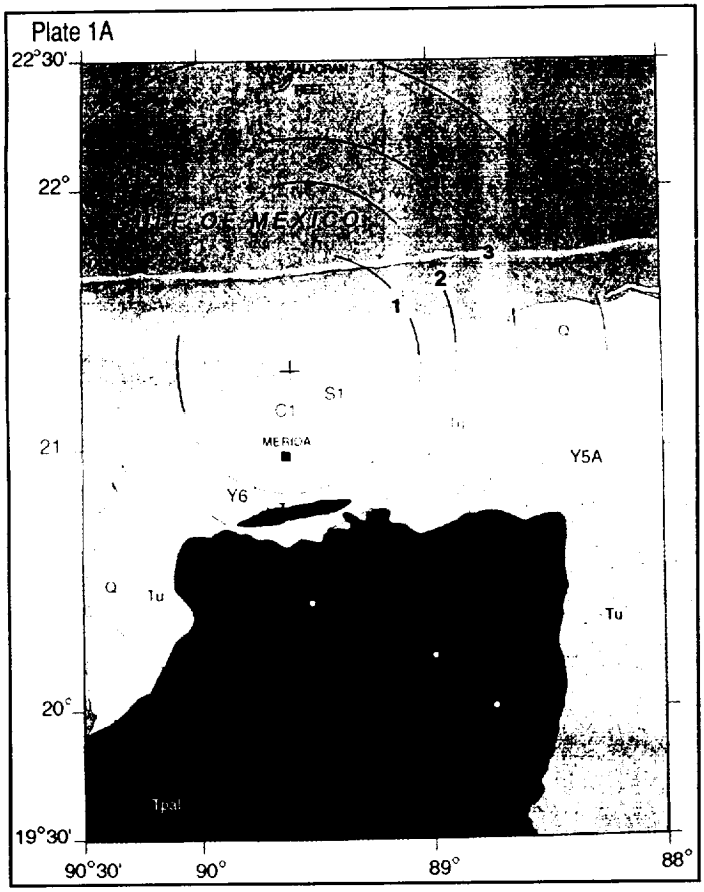
Plate 1A
22°30'
22°
21
20°
19°30'
90°30'
90°
89°
88°
GULF OF MEXICO
1
2
3
Q
Tu
S1
C1
MERIDA
Y5A
Y6
Tpal


Plate 1B


Plate 1C
S1
C1
MERIDA
Y5A
Y6
T1
Y2
Y1

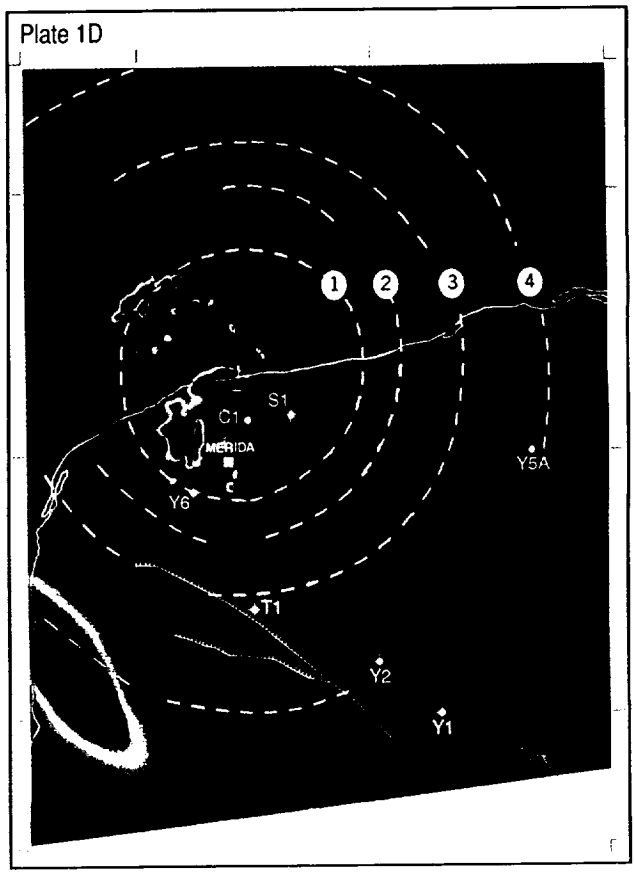
Plate 1D
1
2
3
4
S1
C1
MERIDA
Y5A
Y6
T1
Y2
Y1

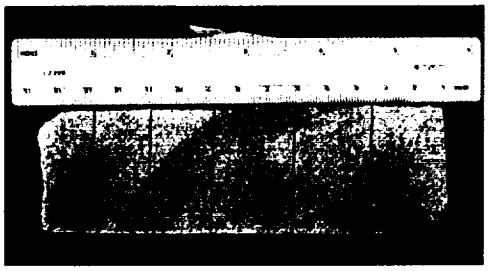

A

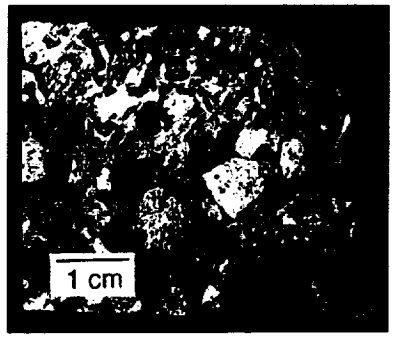

B

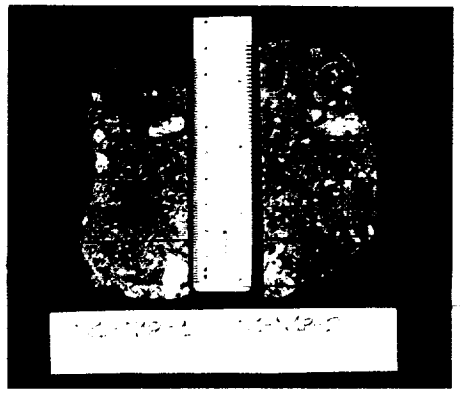

C

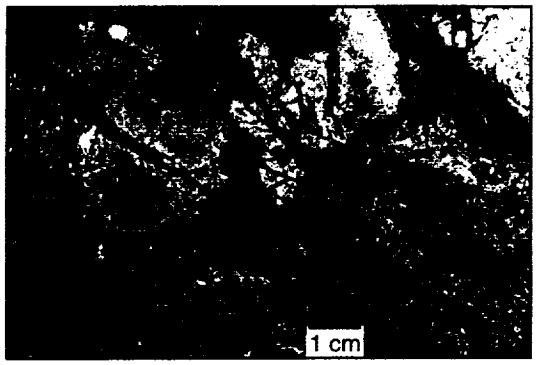

D

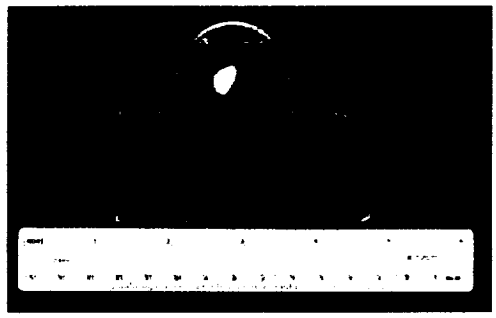

E

F

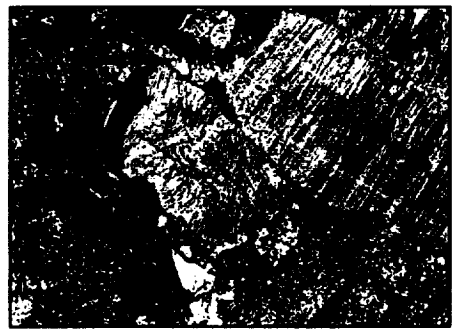

G

H

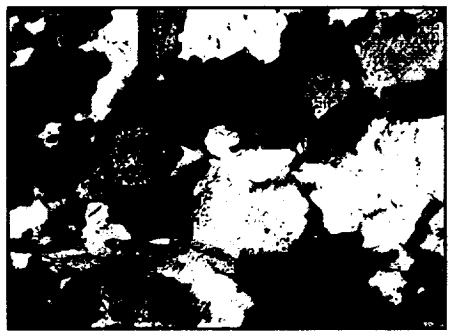

I

J

Plate 2 (caption on page 72)

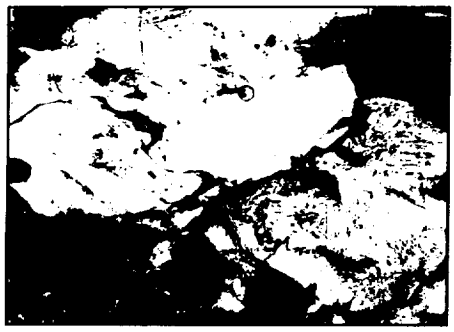

K

L

M

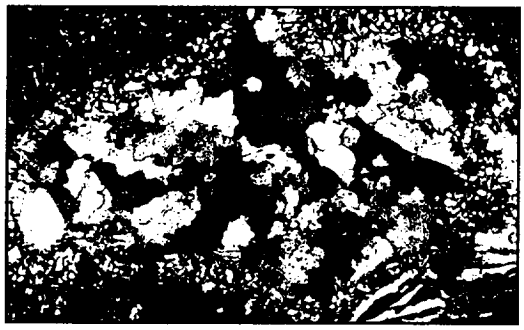

N

O

P

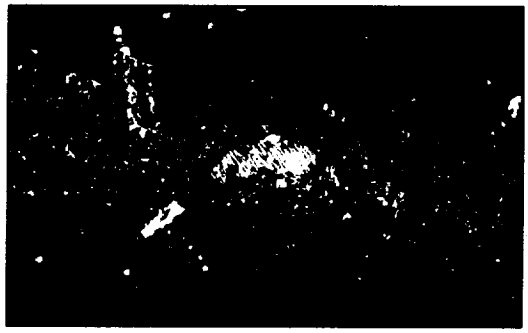

Q

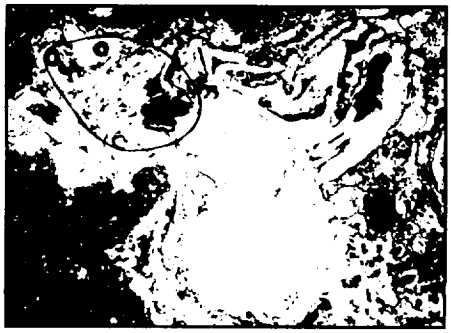

R

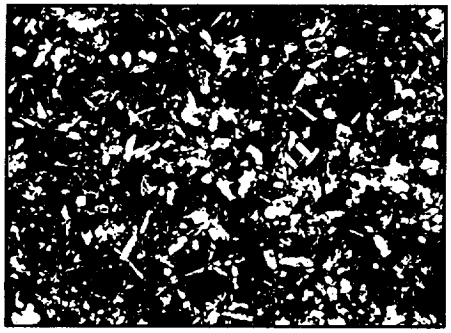

S

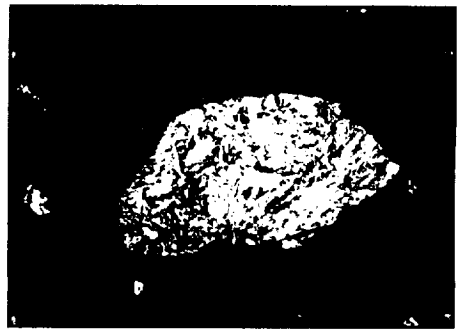

T

Plate 2 (on previous page spread). Photographs and photomicrographs of drill core samples from within the Chicxulub impact basin. **A,** Saw-cut surface of Y6-N13 suevite breccia. **B,** Saw-cut surface of Y6-N14 suevite breccia. **C,** Saw-cut surface of S1-N18 suevite breccia. **D,** Saw-cut surface of Y6-N19 melt matrix breccia. **E,** Saw-cut surface of C1-N10 melt rock. **F and G,** Cross-polarized photomicrographs of Y6-N11 showing shock-deformed quartz clasts with multiple sets of planar deformation features, glass shards, and bioclasts. Width of field is ~4 mm. **H–L,** Cross-polarized photomicrograph of shock-deformed basement clasts from samples Y6-N11, Y6-N14, and S1-N11, showing granitic mineral assemblage and, in some, a primary metamorphic foliation. Width of field is ~2 mm. **K and L,** Cross-polarized photomicrograph of shock-deformed alkali feldspar clasts from Y6-N14. **M,** Cross-polarized photomicrograph of shock-deformed quartz grain from Y6-N19 melt rock showing corona of augite. Width of field is ~1 mm **N,** Cross-polarized photomicrograph of quartz clast with augite corona from Y6-N19 showing ballen structures. These perlitic-fracturelike features result from recrystallization of diaplectic quartz glass. Width of field is ~2 mm. **O,** Cross-polarized photomicrograph of a shock-deformed quartz grain within Y5A-N4 sample of anhydrite-dolomite breccia (Bunte Breccia equivalent). Width of field is ~0.05 mm. **P,** Cross-polarized photomicrograph of a shock-deformed quartz grain from within Y2-N11 sample of anhydrite-dolomite breccia. Width of field is ~0.2 mm. **Q,** Cross-polarized photomicrograph of anhydrite-dolomite breccia sample Y1-N12 showing a shock-deformed quartz grain enveloped within a small pod of partially altered melt rock. Width of field is ~0.2 mm. **R,** Plane-polarized photomicrograph of mineral glass of alkali feldspar composition from Y6-N14 sample. Width of field is ~1.0 mm. **S,** Cross-polarized photomicrograph shows typical igneous texture of C1-N10 with microphenocrysts of plagioclase and augite in a potassium feldspar-rich mesostasis. Width of field is ~9 mm. **T,** Cross-polarized photomicrograph of a clast of anhydrite from Y2-N9 breccia sample. Width of field is ~9 mm.

ACKNOWLEDGMENTS

We thank Antonio Camargo, and Juan Manual Quesada (Pemex), and Gerardo Suárez (Universidad Nacional Autónoma de México) for their assistance and encouragement in this research project. Parts of this research were made possible through research grants provided by the National Aeronautics and Space Administration's Venus Data Analysis Program (to VLS) and Planetary Geology and Geophysics Program (to VLS) and by the National Science Foundation's Continental Dynamics Program. Bevan French and David Fastovsky are gratefully acknowledged for their detailed and constructive reviews, as are Bill Ward, Robbie Herrick, and Gene Perry for their helpful input. Sue Sharpton assisted in manuscript preparation, and Steve Hokanson and Debra Rueb assisted in preparation of artwork. The Lunar and Planetary Institute is operated by Universities Space Research Association under Contract NASW-4574 with NASA. This is Lunar and Planetary Institute Contribution Number 873.

REFERENCES CITED

Alexopoulos, J. S., and McKinnon, W. B., 1994, Large impact craters and basins on Venus, with implications for ring mechanics on the terrestrial planets, *in* Dressler, B. O., Grieve, R. A. F., and Sharpton, V. L., eds., Large meteorite impacts and planetary evolution: Geological Society of America Special Paper 293, p. 29–50.

Alvarez, L. W., Alvarez, W., Asaro, F., and Michel, H. V., 1980, Extraterrestrial cause for the Cretaceous-Tertiary extinction: Science, v. 208, p. 1095–1108.

Antoine, L. A. G., Nicolaysen, L. O., and Niccol, S. L., 1990, Processed and enhanced gravity and magnetic images over the Vredefort structure and their interpretation: Tectonophysics, v. 171, p. 63–74.

Baldwin, R. B., 1963, The measure of the Moon: Chicago, University of Chicago Press, 488 p.

Bishoff, L., and Oskierski, W., 1988, The surface structure of the Haughton impact crater, Devon Island, Canada: Meteoritics, v. 23, p. 209–220.

Bishoff, A., and Stöffler, D., 1981, Thermal metamorphism of feldspar clasts in impact melt rocks from Lappäjarvi crater, Finland [abs]: Lunar and Planetary Science Conference, 12th, Abstracts of Papers: Houston, Texas, Lunar and Planetary Institute, p. 77–79.

Blum, J. D., Chamberlain, C. P., Koeberl, C., Marín, L. E., Schuraytz, B. C., and Sharpton, V. L., 1993, Isotopic comparison of K/T boundary impact glass with melt rock from the Chicxulub and Manson impact structures: Nature, v. 364, p. 325–327.

Bohor, B. F., 1990, Shocked quartz and more: Impact signatures in Cretaceous/Tertiary boundary clays, *in* Sharpton, V. L., and Ward, P. D., eds., Global catastrophes in Earth history: An interdisciplinary conference on impacts, volcanism, and mass mortality: Geological Society of America Special Paper 247, p. 335–342.

Bohor, B. F., Foord, E. E., Modreski, P. J., and Triplehorn, D. M., 1984, Mineralogic evidence for an impact event at the Cretaceous-Tertiary boundary: Science, v. 224, p. 867–869.

Bourgeois, J., Hansen, T. A., Wiberg, P. L., and Kauffman, E. G., 1988, A tsunami deposit at the Cretaceous-Tertiary boundary in Texas: Science, v. 241, p. 567–570.

Byars, C., 1981, Mexican site may be link to dinosaurs disappearance: Houston Chronicle, December 13, p. 1, continued on p. 18.

Camargo, Z., A., and Suárez, R., G., 1994, Evidencia sismica del crater de impacto de Chicxulub [Seismic evidence of the Chicxulub Impact Crater]: Boletín de la Asociación Mexicana de Geofisicos de Exploracion, v. 34, p. 1–28 (in Spanish).

Carstens, H., 1975, Thermal history of impact melt rocks in the Fennoscandian shield: Contributions to Mineralogy and Petrology, v. 50, p. 145–155.

Cornejo-Toledo, A., and Hernandez-Osuna, A., 1950, Las anomalias gravimetricas en la cuenca salina del istmo, planicie costera de Tabasco, Campeche y Pensula de Yucatan: Boletín de la Asociación Mexicana de Geólogos Petroleros, v. 2, p. 453–460.

Croft, S. K., 1981a, The excavation stage of basin formation: A qualitative model, *in* Schultz, P. H., and Merrill, R. B., eds., Multi-ring basins: New York, Pergamon Press, p. 207–225.

Croft, S. K., 1981b, The modification stage of basin formation: Conditions of ring formation, *in* Schultz, P. H., and Merrill, R. B., eds., Multi-ring basins: New York, Pergamon Press, p. 227–257.

Dressler, B. O., 1982, Geology of the Wanapitei Lake area, District of Sudbury: Ontario Geological Survey report, v. 213, 131 p.

Engelhardt, W. v., 1972, Shock produced rock glasses from the Ries crater: Contributions to Mineralogy and Petrology, v. 36, p. 265–292.

French, B. M., and Nielsen, R. L., 1990, Vredefort Bronzite Granophyre:

Chemical evidence for origin as a meteorite impact melt: Tectonophysics, v. 171, p. 119–138.

Grieve, R. A. F., and Ber, T. J., 1994, Shocked lithologies at the Wanapitei impact structure, Ontario, Canada: Meteoritics, v. 29, p. 621–631.

Grieve, R. A. F., and Floran, R. J., 1978, Manicouagan impact melt, Quebec. 2: Chemical interrelations with basement and formational processes: Journal of Geophysical Research, v. 83, p. 2761–2771.

Grieve, R. A. F., Robertson, P. B., and Dence, M. R., 1981, Constraints on the formation of ring impact structures based on terrestrial data, *in* Schultz, P. H., and Merrill, R. B., eds., Multi-ring basins: Proceedings of Lunar and Planetary Science, Volume 12, Part A: New York, Pergamon, p. 37–57.

Grieve, R. A. F., Stöffler, D., and Deutsch, A., 1991, The Sudbury Structure: Controversial or misunderstood?: Journal of Geological Research, v. 96, p. 22, 753, 764.

Hart, R. J., Hargraves, R. B., Andreoli, M. A. G., Tredoux, M., and Doucouré, C. M., 1995, Magnetic anomaly near the center of the Vredefort structure: Implications for impact related magnetic signatures: Geology, v. 23, p. 277–280.

Head, J. W., 1977, Origin of outer rings in lunar multi-ringed basins: Evidence from morphology and ring spacing, *in* Roddy, D. J., Pepin, R. O., and Merrill, R. B., eds., Impact and explosion Cratering: New York, Pergamon Press, p. 563–573.

Hildebrand, A. R., 1992, Geochemistry and stratigraphy of the Cretaceous/Tertiary boundary impact ejecta [Ph.D. thesis]: Tucson, University of Arizona, 358 p.

Hildebrand, A. R., 1993, The Cretaceous/Tertiary boundary impact (or the dinosaurs didn't have a chance): Journal of the Royal Astronomical Society of Canada, v. 87, p. 77–118.

Hildebrand, A. R., and Boynton, W. W., 1990, Proximal Cretaceous-Tertiary boundary deposits in the Caribbean: Science, v. 248, p. 843–847.

Hildebrand, A. R., Penfield, G. T., Kring, D. A., Pilkington, M., Camargo, Z. A., Jacobsen, S., and Boynton, W. V., 1991, A possible Cretaceous-Tertiary boundary impact crater on the Yucatán peninsula, Mexico: Geology, v. 19, p. 867–871.

Hörz, F., and Banholzer, G. S., 1980, Deep-seated target materials in the continuous deposits of the Ries Crater, Germany, *in* Papike, J. J., and Merrill, R. B., eds., Proceedings of the Conference on Lunar Highlands Crust: New York, Pergamon Press, p. 211–231.

Hörz, F., Ostertag, R., and Rainey, D. A., 1983, Bunte Breccia of the Ries: Continuous deposits of large impact craters: Reviews of Geophysics and Space Physics, v. 21, p. 1667–1725.

Howard, K. A., Wilhelms, D. E., and Scott, D. H., 1974, Lunar basin formation and highland stratigraphy: Reviews of Geophysics and Space Physics, v. 12, p. 309–327.

Izett, G. A., 1990, The Cretaceous/Tertiary boundary interval, Raton Basin, Colorado and New Mexico, and its content of shock-metamorphosed minerals: Evidence relevant to the K-T boundary impact-extinction theory: Geological Society of America Special Paper 249, 100 p.

Izett, G. A., Maurrasse, F. J.-M. R., Lichte, F. E., Meeker, G. P., and Bates, R., 1990, Tektites in Cretaceous-Tertiary boundary rocks on Haiti: U.S. Geological Survey Open-File Report OF-90-635, 31 p.

Jansa, L. F., Pe-Piper, G., Robertson, P. B., and Friedenreich, O., 1989, Montagnais: A submarine impact structure on the Scotian Shelf, eastern Canada: Geological Society of America Bulletin, v. 101, p. 450–463.

Jansa, L. F., Aubry, M.-P., and Gradstein, F. M., 1990, Comets and extinctions: Cause and effect? *in* Sharpton, V. L., and Ward, P. D., eds., Global catastrophes in Earth history: An interdisciplinary conference on impacts, volcanism, and mass mortality: Geological Society of America Special Paper 247, p. 223–232.

Jung, K., Shaaf, H., and Kahle, H. G., 1969, Ergebnisse gravimetrischer Messungen im Ries [Results of gravimetric measurements in the Ries]: Geologica Bavarica, v. 61, p. 337–342 (in German).

Kamo, S. L., and Krogh, T. E., 1995, Chicxulub crater source for shocked zircon crystals from the Cretaceous-Tertiary boundary layer, Saskatchewan: Evidence from new U-Pb data: Geology, v. 23, p. 281–284.

Kieffer, S. W., and Simonds, C. H., 1980, The role of volatiles and lithology in the impact cratering process: Reviews of Geophysics and Space Physics, v. 18, p. 143–181.

Koeberl, C., Sharpton, V. L., Schuraytz, B. C., Shirey, S. B., Blum, J. D., and Marín, L. E., 1994, Evidence for a meteoritic component in impact melt rock from the Chicxulub structure: Geochimica et Cosmochimica Acta, v. 58, p. 1679–1684.

Kring, D. A., 1993, The Chicxulub impact event and possible causes of KT boundary extinctions, *in* Boaz, D., and Dornan, M., eds., Proceedings, Annual Symposium of Fossils of Arizona, 1st: Mesa, Arizona, Mesa Southwest Museum and Southwest Paleontological Society, p. 63–79.

Kring, D. A. and Boynton, W. V., 1992, Petrogenesis of an augite-bearing melt rock in the Chicxulub structure and its relationship to K/T impact spherules in Haiti: Nature, v. 358, p. 141–144.

Krogh, T. E., Kamo, S. L., Sharpton, V. L., Marín, L. E., and Hildebrand, A. R., 1993, U-Pb ages of single shocked zircons linking distal K/T ejecta to the Chicxulub crater: Nature, v. 366, p. 731–734.

Lopez-Ramos, E., 1983, Geologia de Mexico (third edition): Mexico City, Universidad Nacional Autónoma de México, p. 269–301 (in Spanish).

Marín, L. E., Sharpton, V. L., Urrutia-Fucugauchi, J., Sikora, P., and Carney, C., 1994, The "Upper Cretaceous Unit" in the Chicxulub multiring basin: New age based on planktic foraminiferal assemblage [abs.], *in* New developments regarding the KT event and other catastrophes in Earth history: Houston, Texas, Lunar and Planetary Institute Contribution 825, p. 77.

Marshall, R. G., 1974, Petrology of subsurface Mesozoic rocks of the Yucatan Platform, Mexico [M.S. thesis]: New Orleans, Louisiana, University of New Orleans, 97 p.

Masaitis, V. L., 1990, Impactites from Popigai Crater, *in* Dressler, B. O., Grieve, R. A. F., and Sharpton, V. L., eds., Large meteorite impacts and planetary evolution: Geological Society of America Special Paper 293, p. 153–162.

Masaitis, V. L., and five others, 1980, The geology of astroblems: Leningrad, Nedra, 231 p. (in Russian).

McIntyre, D. B., 1968, Impact metamorphism at Clearwater Lake, Quebec, *in* French, B. M., and Short, N. M., eds., Shock metamorphism of natural materials: Baltimore, Maryland, Mono Book, p. 363–366.

Melosh, H. J., 1989, Impact cratering: A geological process: New York, Oxford University Press, 245 p.

Melosh, H. J., and McKinnon, W. B., 1978, The mechanics of ringed basin formation: Geophysical Research Letters, v. 5, p. 985–988.

Newsom, H. E., Graup, G., Iseri, D. A., Geissman, J. W., and Keil, K., 1990, The formation of the Ries Crater, West Germany: Evidence of atmospheric interactions during a large cratering event, *in* Sharpton, V. L., and Ward, P. D., eds., Global catastrophes in Earth history: An interdisciplinary conference on impacts, volcanism, and mass mortality: Geological Society of America Special Paper 247, p. 195–206.

Nicolaysen, L. O., 1990, the Vredefort structure: An introduction and a guide to recent literature: Tectonophysics, v. 171, p. 1–6.

Penfield, G. T., and Camargo Z., A., 1981, Definition of a major igneous zone in the central Yucatán platform with aeromagnetics and gravity, *in* Technical Program, Abstracts and Bibliographies, Society of Exploration Geophysicists, 51st Annual Meeting, Tulsa, Oklahoma, Society of Exploration Geophysicists, p. 37.

Phinney, W. C., Simonds, C. H., Cochran, A., and McGee, P. E., 1978, West Clearwater Quebec, impact structure: Part II: Petrology: Proceedings, Lunar and Planetary Science Conference, 9th, Volume 2: New York, Pergamon Press, p. 2659–2693.

Pike, R. J., and Spudis, P. D., 1987, Basin-ring spacing on the Moon, Mercury, and Mars: Earth, Moon, and Planets, v. 39, p. 129–194.

Pilkington, M., and Grieve, R. A. F., 1992, The geophysical signature of terrestrial impact craters: Reviews of Geophysics, v. 30, p. 161–181.

Pilkington, M., Hildebrand, A. R., and Ortiz-Aleman, C., 1994, Gravity and magnetic field modeling and structure of the Chicxulub Crater, Mexico:

Journal of Geophysical Research, v. 99, p. 13147–13162.

Pohl, J., Stöffler, D., Gall, H., and Ernstson, K., 1977, The Ries impact crater, *in* Roddy, D. J., Pepin, R. O., and Merrill, R. B., eds., Impact and explosion cratering: New York, Pergamon Press, p. 343–404.

Pohl, J., Eckstaller, A., and Robertson, P. B., 1988, Gravity and magnetic investigations in the Haughton impact structure, Devon Island, Canada: Meteoritics, v. 23, p. 235–238.

Pope, K. O., Ocampo, A. C., and Duller, C. E., 1991, Mexican site for the K/T Crater?: Nature, v. 351, p. 105.

Pope, K. O., Ocampo, A. C., and Duller, C. E., 1993, Surficial geology of the Chicxulub impact crater Yucatán, México: Earth, Moon and Planets, v. 63, p. 93–104.

Redeker, H.-J., and Stöffler, D., 1988, The allochthonous polymict breccia layer of the Haughton impact crater, Devon Island, Canada: Meteoritics, v. 23, p. 185–196.

Roest, W., and Pilkington, M., 1994, Restoring post-impact deformation at Sudbury: A circular argument: Geophysical Research Letters, v. 21, p. 959–962.

Schaber, G. G., and nine others, 1992, Geology and distribution of impact craters on Venus: What are they telling us?: Journal of Geophysical Research, v. 97, p. 13257–13301.

Schmidt, R. M., and Housen, K. R., 1987, Some recent advances in scaling of impact and explosion cratering: International Journal of Impact Engineering, v. 5, p. 543–560.

Schultz, P. H., 1976, Moon morphology: Austin, University of Texas Press, 926 p.

Schuraytz, B. C., and Sharpton, V. L., 1993, Chicxulub—K/T melt complexities: Nature, v. 362, p. 503–504.

Schuraytz, B. C., and Sharpton, V. L., 1994, Siderophile-element distribution in Chicxulub melt rocks: Forensic chemistry on the KT smoking gun, *in* New developments regarding the KT event and other catastrophes in Earth history [abs.]: Houston, Texas, Lunar and Planetary Institute Contribution 825, p. 106–108.

Schuraytz, B. C., Sharpton, V. L., and Marín, L. E., 1994, Petrology of impact-melt rocks at the Chicxulub multiring basin, Yucatán, Mexico: Geology, v. 22, p. 868–872.

Scott, D., and Hajnal A., 1988, Seismic signature of the Haughton structure: Meteoritics, v. 23, p. 239–247.

Sharpton, V. L., and Ward, P. D., eds., 1990, Global catastrophes in Earth history: An interdisciplinary conference on impacts, volcanism, and mass mortality: Geological Society of America Special Paper 247, 631 p.

Sharpton, V. L., Schuraytz, B. C., Burke, K., Murali, A. V., and Ryder, G., 1990a, Detritus in K/T boundary clays of western North America: Evidence against a single oceanic impact, *in* Sharpton, V. L., and Ward, P. D., eds., Global catastrophes in Earth history: An interdisciplinary conference on impacts, volcanism, and mass mortality: Geological Society of America Special Paper 247, p. 349–359.

Sharpton, V. L., Schuraytz, B. C., and Jones, J., 1990b, Arguments favoring a single continental impact at the KT boundary: Meteoritics, v. 25, p. 408–409.

Sharpton, V. L., and five others, 1992, New links between the Chicxulub impact structure and the Cretaceous/Tertiary boundary, Nature, v. 359, p. 819–821.

Sharpton, V. L., and 9 others, 1993, Chicxulub multi-ring impact basin: Size and other characteristics derived from gravity analysis: Science, v. 261, p. 1564–1567.

Sharpton, V. L., Marín, L. E., and Schuraytz, B. C., 1994a, The Chicxulub multiring impact basin: Evaluation of geophysical data, well logs, and drill core samples [abs.], *in* New developments regarding the KT event and other catastrophes in Earth history: Houston, Texas, Lunar and Planetary Institute Contribution 825, p. 108–110.

Sharpton, V. L., Marín, L. E., and Schuraytz, B. C., 1994b, Constraints on excavation and mixing during the Chicxulub impact event [abs.], *in* 25th Lunar and Planetary Science Conference: Houston, Texas, Lunar and Planetary Institute, p. 1255–1256.

Shoemaker, E. M., Wolfe, R. F., and Shoemaker, E. S., 1990, Asteroid and comet flux in the neighborhood of Earth, *in* Sharpton, V. L., and Ward, P. D., eds., Global catastrophes in Earth history: An interdisciplinary conference on impacts, volcanism, and mass mortality: Geological Society of America Special Paper 247, p. 155–170.

Simonds, C. H., Phinney, W. C., McGee, P. E., and Cochran, A., 1978, West Clearwater, Quebec impact structure, Part I: Field geology, structure and bulk chemistry: Proceedings, Lunar and Planetary Science Conference, 9th, Volume 2: New York, Pergamon Press, p. 2633–2658.

Sky and Telescope, 1982, Possible Yucatan impact basin: Sky and Telescope, v. 63, p. 249–250.

Spudis, P. D., 1993, The geology of multi-ring impact basins: Cambridge, Cambridge University Press, 263 p.

Spudis, P. D., Reisse, R. A., and Gillis J. J., 1994, Ancient multiring basins on the Moon revealed by Clementine laser altimetry: Science, v. 266, p. 1848–1851.

Stepto, D., 1990, The geology and gravity field in the central core of the Vredefort structure: Tectonophysics, v. 171, p. 75–103.

Stöffler, D., 1977, Research drilling Nördlingen 1973: Polymict breccias, crater basement, and cratering model of the Ries impact structure: Geologica Bavarica, v. 75, p. 443–458.

Stöffler, D., and Langenhorst, F., 1994, Shock metamorphism of quartz in nature and experiment, I: Basic observation and theory: Meteoritics, v. 29, p. 155–181.

Stöffler, D., Ewald, U., Ostertag, R., and Reimold, W. U., 1977, Ries deep drilling, I: Composition and texture of polymict breccias: Geologica Bavarica, v. 75, p. 163–189.

Swisher, C. C., III, and 11 others, 1992, Coeval $^{40}Ar/^{39}Ar$ ages of 65.0 million years ago from Chicxulub melt rock and Cretaceous-Tertiary boundary tektites: Science, v. 257, p. 954–958.

Urrutia-Fucugauchi, J., Marín, L., and Sharpton, V. L., 1994, Reverse polarity magnetized melt rocks from the Cretaceous/Tertiary Chicxulub structure, Yucatan peninsula, Mexico: Tectonophysics, v. 237, p. 105–112.

Vickery, A. M., and Melosh, H. J., 1990, Atmospheric erosion and impactor retention in large impacts, with application to mass extinctions, *in* Sharpton, V. L., and Ward, P. D., eds., Global catastrophes in Earth history: An interdisciplinary conference on impacts, volcanism, and mass mortality: Geological Society of America Special Paper 247, p. 289–300.

Viniegra O., F., 1981, Great carbonate bank of Yucatan, southern Mexico: Journal of Petroleum Geology v. 3, p. 247–278.

Ward, W. C., Weidie, A.E., and Back, W., 1985, Geology and hydrogeology of the Yucatan and Quaternary geology of northeastern Yucatan Peninsula: New Orleans, New Orleans Geological Society Publications, 160 p.

Ward, W. C., Keller, G., Stinnesbeck, W, and Adatte, T., 1995, Yucatan subsurface stratigraphy: Implications and constraints for the Chicxulub impact: Geology, v. 23, 873–876.

Weidie, A. E., 1985, Geology of Yucatan Platform, *in* Ward, W. C., Weidie, A. E., and Back, W., eds, Geology and hydrogeology of the Yucatan and Quaternary geology of northeastern Yucatan Peninsula: New Orleans, New Orleans Geological Society Publications, p 1–19.

Weidie, A. E., Ward, W. C, and Marshall, R. M., 1978, Geology of Yucatan Platform, *in* Ward, W. C., and Weidie, A. E., eds., Geology and hydrogeology of northeastern Yucatan: New Orleans, New Orleans Geological Society Publications, p. 3–29.

Weissman, P. R., 1988, Terrestrial impact rates for long and short-period comets, *in* Silver, L. T., and Schultz, P. H., eds., Geological implications of impacts of large asteroids and comets on the Earth: Geological Society of America Special Paper 190, p. 15–24.

Wilhelms, D. E., 1987, The geologic history of the Moon: U.S. Geological Survey Professional Paper 1348, 328 p.

Zuber, M. T., Smith, D. E., Lemoine, F. G., and Neumann, G. A., 1994, The shape and internal structure of the Moon from the Clementine Mission: Science, v. 266, p. 1839–1843.

Manuscript Accepted by the Society September 14, 1995

Printed in U.S.A.